

FMH606 Master's Thesis 2024  
Energy and Environmental Technology

# **CPFD simulation of fluidized bed-based gas cooler**

Md Al-Amin

Faculty of Technology, Natural sciences and Maritime Sciences  
Campus Porsgrunn

**Course:** FMH606 Master's Thesis, 2024

**Title:** CPFD simulation of fluidized bed-based gas cooler.

**Number of pages:** 77.

**Keywords:** Fluidization, fluidized bed, bubbling fluidized bed, minimum fluidization velocity, minimum bubbling velocity, terminal velocity, CPFD simulation, gas cooler, heat transfer in fluidized bed, cooling load, coolant flowrate.

<b>Student:</b>	Md Al-Amin
<b>Supervisor:</b>	Chameera Jayarathna Burkhard Sachs Janitha Bandara
<b>External partner:</b>	Hydro Aluminium AS

**Summary:**

Fluidization technology is extensively used in numerous industries for various processes including waste-to-energy conversion, chemical synthesis, granulation, drying etc. Fluidized bed systems are used for these applications, offering even heat distribution and effective energy transmission for thermal systems. The addition or extraction of heat is essential for accomplishing desired reactions and controlling the entire process.

One of the leading industries is engaged in performing research and development (R&D) operations to efficiently capture carbon dioxide (CO<sub>2</sub>). In this process, the exhaust gases need to be cooled down from a temperature of 400 °C to 100 °C or lower utilizing an existing coolant. This study aims to examine and simulate the available data using CPFDF Barracuda VR<sup>®</sup> to create a more accurate and realistic model of a gas cooler.

This thesis aims to study literature, developing a bubbling fluidized bed, computing the cooling load and tube length, finding the flowrate of the coolant to design an optimal gas cooler according to the fluidized bed principle, where cooling tubes are immersed in the dense region of the fluidized bed. The hot gas is introduced from the bottom, and it cools down because of heat exchange between the coolant and the fluidization gas, as well as between the coolant and the solid particles in the bed.

CPFDF Barracuda VR<sup>®</sup> simulation version 23.1.0 and Techplot 360 is used for simulation and post processing of data. Thermal calculation of the gas cooler is done by NTU method.

The findings of this study shows that the cooling load obtained from calculation is 742.6 J/s which is very close to the simulation result 750 J/s. The heat transfer area, the internal cooling tubes length and coolant flow rate is found to be approximately 49500 mm<sup>2</sup>, 3221 mm and 12.78 kg/h respectively and vertical tubes shows better performance compared to horizontal tubes alignment.

# Preface

I am very delighted and grateful to Almighty God for his Marcy and blessing that help me to complete the task.

This thesis report has been written as a part of the subject FMH606 master's thesis at the University of South Eastern Norway, spring semester 2024.

First and foremost, I would like to express my deepest gratitude to my supervisor, Chameera Jayarathna from USN and Burkhard Sachs, Janitha Bandara and their team from Hydro Aluminium AS for their guidance, recommendation, and continuous support on the journey. Their collaboration and constrictive feedback make me enable to think deeply and shape the thesis to fulfill the objectives.

I am also immensely grateful to the faculty and staff of the university. Their supportive hand helps me to understand and implement the newly learn software in effective way.

I want to mention the quick response team of CPF D Barracuda VR<sup>®</sup> support center for the instructions which was remedy for problems arises during the use of software.

On a personal note, I am deeply indebted to my family and friends for their unwavering support, patience and encouragement which have been a source of strength during my journey.

Porsgrunn, 30-05-2024

Md Al-Amin

# Contents

<b>1</b>	<b>Introduction .....</b>	<b>13</b>
1.1	Background .....	13
1.2	Objectives .....	16
1.3	Overview of report .....	16
<b>2</b>	<b>Literature review .....</b>	<b>17</b>
2.1	Fluidization techniques .....	17
2.2	Fluidization regimes .....	18
2.3	Particles classification .....	19
2.4	Particle size distribution .....	20
2.5	Bubbling fluidization bed .....	20
2.5.1	<i>Lower zone.....</i>	<i>21</i>
2.5.2	<i>Upper zone.....</i>	<i>21</i>
2.6	Gas distributor design.....	21
<b>3</b>	<b>Theory .....</b>	<b>25</b>
3.1.1	<i>Minimum fluidization velocity .....</i>	<i>25</i>
3.1.2	<i>Minimum bubbling velocity.....</i>	<i>26</i>
3.1.3	<i>Terminal velocity.....</i>	<i>26</i>
3.1.4	<i>Mean diameter .....</i>	<i>27</i>
3.1.5	<i>Other particle properties .....</i>	<i>27</i>
3.2	Grid generation .....	28
3.3	CPFD terminology.....	29
3.4	Governing equation .....	29
3.5	Thermal modeling in CPFD.....	31
3.5.1	<i>Convective fluid to wall heat transfer mechanism .....</i>	<i>31</i>
3.5.2	<i>Convective fluid to particle heat transfer mechanism .....</i>	<i>32</i>
3.5.3	<i>Radiation thermal flow.....</i>	<i>33</i>
3.5.4	<i>Available model for drag force and drag model selection.....</i>	<i>34</i>
<b>4</b>	<b>Methodology.....</b>	<b>37</b>
4.1	Thermal approach.....	37
4.2	Cooling load .....	38
4.3	Fluidized bed approach.....	39
4.4	Thermal flow consideration .....	40
4.5	Internal cooling tube design .....	40
4.6	Isothermal simulation for optimizing bed properties.....	42
4.6.1	<i>Simulation setup .....</i>	<i>42</i>
4.6.2	<i>Simulation cases for isothermal.....</i>	<i>46</i>
4.7	Thermal Simulation for optimizing cooling capacity .....	47
4.7.1	<i>Simulation setup .....</i>	<i>47</i>
4.7.2	<i>Simulation cases for non-isothermal.....</i>	<i>48</i>
<b>5</b>	<b>Result and discussion .....</b>	<b>49</b>
5.1	Particles size distribution .....	49
5.2	Fluidized gas properties .....	50
5.3	Fluidized gas velocity .....	50
5.3.1	<i>Bed diameter, height, bottom surface area, bed static volume and amount of bed material calculation.....</i>	<i>51</i>
5.4	Cooling performance calculation .....	51

5.5 H/D ratio of the bed.....52

5.6 Optimum superficial velocity.....55

5.7 Optimum area.....57

5.8 Heat transfer performance.....58

    5.8.1 Vertical cooling tubes performance.....58

    5.8.2 Horizontal cooling tubes performance.....64

6 Conclusion .....67

References.....68

Appendices.....71

    Appendix A.....71

    Appendix B.....72

    Appendix B.....73

    Appendix C.....74

    Appendix D.....75

## List of figures

Figure 1.1: Overview of the research and application of fluidized bed heat exchangers [4].	14
Figure 1.2: Advantages and related application fields of fluidized bed heat exchangers [4].	14
Figure 1.3: Diagram of gas cooler (source: MT-04-24 thesis task description).	15
Figure 2.1: Fluidization technique.	17
Figure 2.2: Fluidization bed regimes [10].	18
Figure 2.3: Classification of particles in 1973 by Geldart [13].	19
Figure 2.4: Dense phase and lean phase of particles in bubbling fluidized bed [10].	20
Figure 2.5: Gas distributors (a) sandwiching perforated plates;(b) staggered perforated plates; (c) dished perforated plate; (d) grate bars [10].	21
Figure 2.6: Gas distributors (a) porous plate types; (b) nozzle type (c) bubble Cap type still nozzle type [10].	22
Figure 2.7: : Babbles behaviors during fluidization (a) porous plate; (b) perforated plate; (c) nozzle-type tuyere; (d) bubble cap tuyere [10].	22
Figure 3.1: Various particle properties [24].	28
Figure 3.2: Steps of gridding, meshing and analysis in CPFDF [26].	28
Figure 3.3: 2D and 3D mesh in CPFDF [26].	29
Figure 4.1: Overview of methodology.	37
Figure 4.2: Vertical cooling tubes alignment (a) x-y-z view, (b) x-z plan, (c) x-z plan.	41
Figure 4.3: Horizontal cooling tubes alignment (a) x-y-z view, (b) x-z plan, (c) x-z plan.	41
Figure 4.4: (a) CAD model, (b) flux plane, (c) data points, (d) combined grid and CAD model.	42
Figure 4.5: Uniform grid setup and grid checking on Barracuda VR®.	43
Figure 4.6: Global settings setup.	43
Figure 4.7: Particle properties editor (a) & (b).	44
Figure 4.8: Fluid initial conditions and particle initial conditions in bed.	44
Figure 4.9: Pressure boundary setting.	45
Figure 4.10: Flow boundary setting.	45
Figure 4.11 Time-control setting.	45
Figure 4.12: Global setting for non-isothermal condition.	47
Figure 4.13: Thermal cooling tube setting.	48
Figure 5.1: Particle size distribution.	49
Figure 5.2: Particles distributions throughout the bed.	52
Figure 5.3: Particle out flow for simulation_A01, A02, A03, A04 and A05.	54

Figure 5.4: Time-integrated particle mass of all species. ....54

Figure 5.5: Particle out flow for simulation\_B01, B02, B03, B04 and B05.....56

Figure 5.6: Cumulative particle mass out flow for 300 s.....57

Figure 5.7: Particle out flow for simulation\_C01, C02, C03, and C04. ....58

Figure 5.8: Heat transfer rate for vertical tubes. ....59

Figure 5.9: Average temperature at top of the gas cooler.....60

Figure 5.10: Time integrated heat transfer of cooling tubes.....60

Figure 5.11: Gas pressure at top of cylinder. ....61

Figure 5.12 : fluid temperature profile over time. ....61

Figure 5.13: Particle temperature changed over time. ....62

Figure 5.14: Simulation outputs (a) heat transfer rate of system, (b) Gas temperature at outlet, (c) time integrated heat transfer (d) pressure of gas. ....63

Figure 5.15: Simulation\_V3 (a) heat transfer rate, (b) fluid temperature, (c) Time integrated heat transfer, (d) time integrated mass out flow at top. ....64

Figure 5.16 Simulation output of horizontal tubes (a) heat transfer rate, (b) fluid temperature at top, (c) time integrated heat transfer. ....65



**List of Tables**

Table 4.1: Simulation parameters value for optimizing H/D ratio. ....	46
Table 4.2: Simulation parameters value for optimizing superficial velocity. ....	46
Table 4.3: Simulation parameters value for optimizing bottom surface area of cylinder. ....	46
Table 4.4: Simulation cases for horizontal cooling tube in the bed. ....	48
Table 4.5: simulation cases for horizontal cooling tube in the bed. ....	48
Table 5.2: Carbon-di-oxide properties calculated according to appendix B. ....	50
Table 5.1: Fluidized bed properties. ....	50
Table 5.3: Thermal calculation of various parameters. ....	51

# Nomenclature

Symbol	Description	Unit
$u_{mf}$	Minimum fluidized velocity	m/s
$F_D$	Drag force	N
$\Delta p_{mf}$	Pressure drop	pa
$A$	Cross-sectional area	m <sup>2</sup>
$\rho_s$	Density of solid	kg/m <sup>3</sup>
$\rho_f$	Density of fluid	kg/m <sup>3</sup>
$\varepsilon_{mf}$	Void fraction at minimum fluidization	-
$g$	Gravitational force	m/s <sup>2</sup>
$dp$	Average particle diameter	$\mu\text{m}$
$\mu$	Viscosity of gas	N.s/m <sup>2</sup>
$Ar$	Archimedes' number	-
$\phi_s$	Particle sphericity	-
$u_{mb}$	Minimum bubbling velocity	m/s
$u_t$	Terminal velocity	m/s
$u_t^*$	Dimensionless velocity	-
$d_p^*$	Dimensionless diameter of particles	-
$(Q_{overall})$	Total heat transfer	J
$Q_{walls}$	Heat transfer of tube surface	J
$Q_{bed}$	Heat transfer between fluidized particle/gas medium	J
$\dot{m}_{CO_2}$	Mas flowrate of Gas (CO2)	kg/s
$C_{p,CO_2}$	Heat Capacity of Carbon-di-oxide	J/kg.K

		Nomenclature
$\dot{m}_{water}$	Mass flowrate of Coolant (water)	kg/s
$C_{p,water}$	Heat Capacity of water	J/kg.K
$\epsilon$	Effectiveness of heat exchanger	-
$Q_{max}$	Maximum heat transfers possible	J
$C_{min}$	Minimum Heat capacity	J/kg.K
$C_{max}$	Minimum Heat capacity	J/kg.K
$C_{cold}$	Heat Capacity of coolant	J/kg.K
$C_{hot}$	Heat Capacity of gas	J/kg.K
$A_{tube}$	Surface area of cooling tubes	$m^2$
$h$	Overall heat transfer coefficient	$W/m^2.K$
$l$	Length of tubes	m
$r$	Radius of tube	m
$u_{sf}$	Superficial gas velocity	m/s
$\dot{v}_f$	Volumetric flowrate of gas	m/s
$A_{cylinder's\ bottom}$	Bottom surface area of the cylinder	$m^2$
$H_{BED}$	Static bed height.	m
$M_{FB}$	Mass of the particles in the bed	kg
$V_{FB}$	Volume of bed	$m^3$

**Abbreviations:**

Symbol	Description
ASTM	American society for testing materials
BFBC	Bubbling fluidized bed combustion
CFD	Computational fluid dynamics
CFB	Circulating fluidized bed
CFBC	Circulating fluidized bed combustion
CPFD	Computational particle fluid dynamics
MFV	Minimum fluidization velocity
PSD	Particle size distribution

# 1 Introduction

Modern world facing one of its critical problems of rising temperature mostly causes by the greenhouse gases emitting by industrial activities as well as other sources, many countries agreed on carbon neutral peak by controlling the emission of gasses and efficient use of energy. Effective utilization of energy is essential in the current industrial context, influencing both financial feasibility and ecological durability. Industrial operations consume significant quantities of energy, emphasizing the need for optimization to achieve cost reduction and environmental responsibility. This thesis investigates techniques for enhancing energy efficiency by analyzing bubbling fluidized bed systems as a case study. These systems are very adaptable and efficient for investigating methods to reduce energy use while optimizing performance of a process.

## 1.1 Background

Fluidization technology is very useful in many industrial applications. Various industrial process including waste to energy conversion, chemical synthesis, granulation, drying, agriculture, chemical looping, biomass gasification, pyrolysis, etc. are carried out in fluidized bed reactors [1]. One of the most important applications of fluidization bed is as heating or cooling system for the process due to having almost uniform heat distribution all over the bed [2]. Energy transfer from solid to gas phase or two-phase mixture to heating or cooling medium is a particularly important factor for fluidized bed reactor to control reactions by achieving thermal control of reactor. Most of engineering solutions can be gained by heat addition or extraction on the process [3].

Fluidized bed heat exchanger is one of the good choices for its highly efficient heat transfer performance and excellent anti-fouling characteristics [4]. In the United States in the 1960s, the fluidized bed heat exchanger was used for high-temperature seawater desalination [5]. The applications of this technology was further developed and extended to other sectors like geothermal, desalination, and wastewater treatment as well as others industrial scopes in various countries in 1970s to next [6].

Bubbling fluidized bed technology was first used for gasification in 1921. Work on bubbling fluidized bed combustion (BFBC) technology started in the 1950s, prior to circulating fluidized bed combustion (CFBC). While CFBC plants are more common, BFBC designs are still sold for specialized applications. BFBC plants are water-wall constructions with refractory lining. Early designs had in-bed heat transfer tubing, but this practice has stopped due to high metal loss. Instead, bed temperature is controlled by adjusting air distribution, and all heat is removed by water walls and convection. BFBC units have a lower fluidizing velocity than CFBC units, resulting in less elutriation and no recycle of solids. BFBC is ideal for burning high moisture fuels and is cost-effective for small units. CFBC plants are preferred for larger quantities of better-quality fuels [7].

Following figure 1.1 shows the overview of research progress of fluidized bed application in heat exchangers from 1996 to 2020.

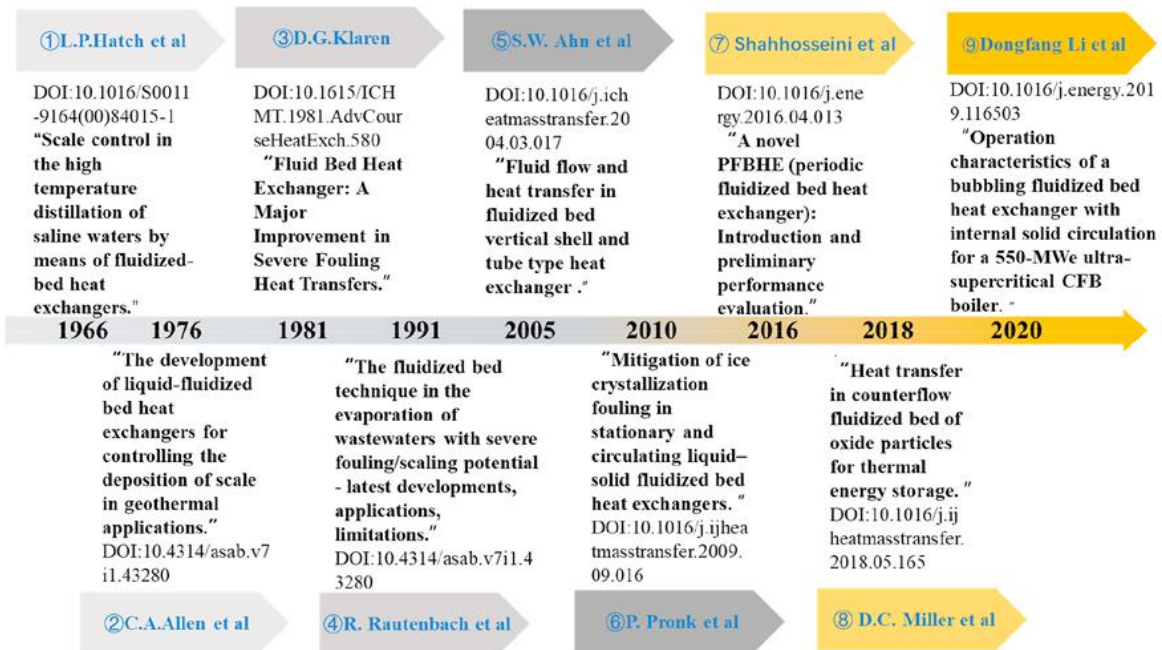


Figure 1.1: Overview of the research and application of fluidized bed heat exchangers [4].

The following figure 1.2 shows an overview of application, advantages, effective parameters and two categories of heat exchangers with some examples of each. This shows the wide range of applications of the heat exchangers such as pharmacy, sugar manufacturing, waste heat recovery etc. [4]. Two flow categories are also shown in the figure where liquid -solid two flow is like the flow in this study.

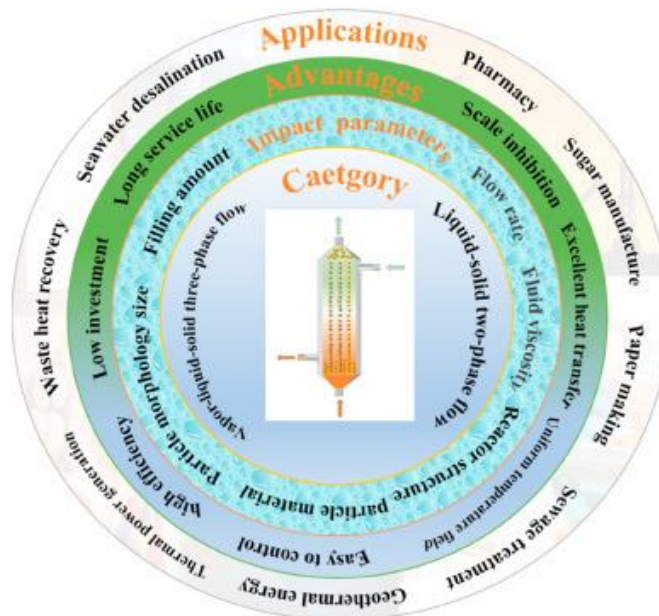


Figure 1.2: Advantages and related application fields of fluidized bed heat exchangers [4]

## 1 Introduction

Although sophisticated technology is used to produce aluminum metal that leads lower carbon dioxide emission, still have remarkable impact on environment and further research going on to reduce more. Aluminum plays an important part in various technologies that are essential for the transition towards clean energy. However, it is also a major contributor to CO<sub>2</sub> emissions, releasing around 270 million metric tons of direct CO<sub>2</sub> emissions in 2022. This accounts for almost 3% of the global direct industrial CO<sub>2</sub> emissions [8]. This study aims to investigate designing such a cooler which will be efficient to cool a stream of carbon di oxide (CO<sub>2</sub>) produced in the industry for further treatment. The heat exchanging cooling tube emerging in the fluidized bed dense phase is considered.

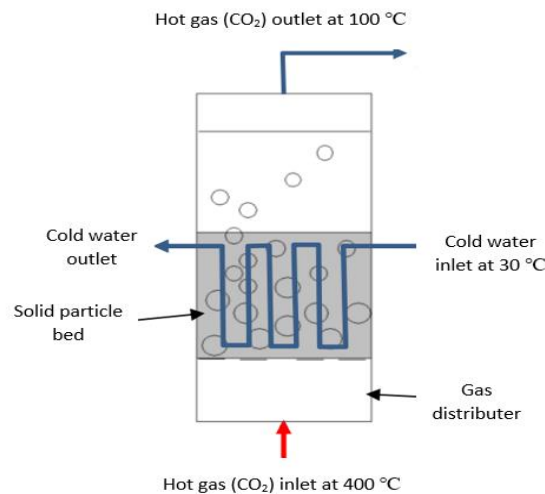


Figure 1.3: Diagram of gas cooler (source: MT-04-24 thesis task description).

Computational Particle Fluid Dynamics (CPFD) is one of the most efficient techniques for solving mass, momentum, and energy conservation equations in complex circumstances. CPFD is a computer-based simulation technique used to investigate fluid flow and related phenomena. It is versatile, with applications in both the industrial and non-industrial sectors. Computational Fluid Dynamics (CFD) analyses are widely used in aerodynamics and hydrodynamics to calculate lift and drag, as well as field parameters like pressures and velocities. These analyses have the potential to save significant time in the design process and are less expensive than standard data collecting testing. However, physical examination cannot be completely removed.

Some of the primary advantages of using Computational Particle Fluid Dynamics (CPFD) are [9]:

- Cost saving
- Time saving
- Computer-based testing reduces costs by eliminating the need for physical prototypes.
- This is a very useful tool to increase accuracy of calculation and prediction of flow behavior.

## 1.2 Objectives

The purpose of this thesis is to study the previous work done by others to design an effective cooler to extract heat from a gas flow stream by using a fluidized bed. The expectation of the work can be pointed out as follows:

- Design a bubbling fluidized bed considering given data and assumptions based on the literature available.
- Finding the heat transfer and calculate the cooling load, heat transfer area, coolant flowrate as well as the tube length of heat exchanger.
- Study several geometrical designs to find the best construction.
- CPFDF simulation of considered cases to fit the most realistic design.

## 1.3 Overview of report

The thesis report is structured according to the following chapter to fulfill the objectives of work. The first chapter describes the introduction which contains a brief background and targets of thesis. Chapter 2 provides literature study for the task. Various parameters and theory are discussed in chapter 3. Computational Particle Fluid Dynamics (CPFDF) terminology and equations and drag model related to the topics are also covered by chapter 3. The methodology of the task is given in chapter 4. Chapter 5 includes the result and discussion part of the thesis. Conclusion and future extension of the task are pointed out in chapter 6.



## 2 Literature review

Fluidization refers to the process by which a bed of solid particles becomes a suspended mass with fluid like characteristics and behaves like a fluid. A liquid or gas is used to pass through the bed of particles where the fluid uplifts the solid particles and collectively work as fluid [10]. Fluidization is a very useful technique for handling particles in industries.

The effectiveness of fluidized bed relies on various factors, such as size, density, and shape, the compositions of the mixture, the gas velocity during operation, the rate of solid flow into the fluidizing column, the height of the bed, and other geometrical parameters of the fluidized bed [11].

### 2.1 Fluidization techniques

The fluidization process involves the upward flow of fluid through a bed of small particles and particles fluidized due to upward movement of gas. The upward-flowing gas provides sufficient drag forces on particles to counterbalance the gravitational force acting downwards on the particles. Simultaneously, particles exert drag forces on flowing fluid that are both equal and opposite magnitude. The drag forces exerted on the particles have an impact on the local gas velocity [12]. When the flow rate is low, gas that is moving upwards is unable to pass through the empty spaces between stationary particles, also known as fixed beds. As the flow rate increases, the particle bed undergoes expansion. If the flow rate is slightly increased over a particular threshold, the gas that is going upwards will disperse all the particles. When the compressive force between particles tend to exist, and the pressure drop at any given segment of the bed is equivalent to the combined weight of the fluid and particles, the bed has undergone fluidization [10].

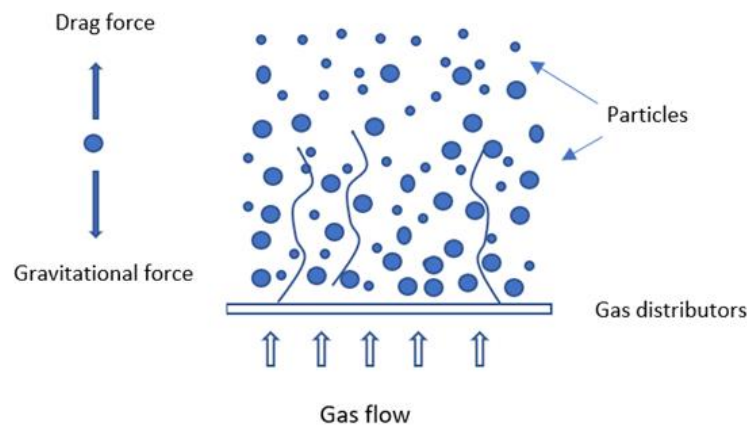


Figure 2.1: Fluidization technique.

## 2.2 Fluidization regimes

The behaviors of the fluidized bed can vary based on several characteristics, including fluid velocity, particle size, and particle properties. Different fluidization regimes can be observed depending on these parameters.

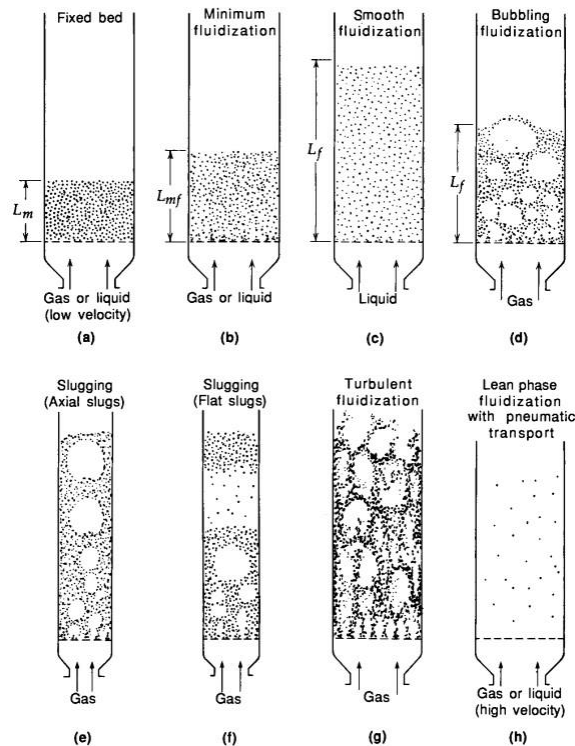


Figure 2.2: Fluidization bed regimes [10].

**Fixed bed:** A fixed bed refers to a reactor or unit operation where a bed of solid particles, catalysts, or adsorbents stays stationary while fluids (such as gases or liquids) flow through it [10].

**Minimum fluidization:** Minimum fluidization is the point at which, when a fluid (gas or liquid) is carried through solid particles in a bed at a specific velocity, the solid particles begin to behave like a fluid. The pressure decrease throughout the bed becomes continuous at this stage [10].

**Smooth or homogenous fluidization:** When there are no visible voids or channels and all the particles in a bed are fluidized uniformly, it is referred to as smooth or homogeneous fluidization. Heat transfer and mixing are consistent as a result [10].

**Bubbling fluidization:** The upward fluid flow causes bubbles to form inside the bed in this type of fluidization. Particles travel within and around the localized spaces that these bubbles produce in the bed [10].

**Slugging:** The term "slugging" describes large agglomerations or "slugs" of particles that arise from the uneven flow of particles in a fluidized bed [10].

**Turbulent fluidization:** Turbulent fluidization happens at higher fluid speeds than smooth

fluidization. In this regime, the fluid flow becomes turbulent, which increases mixing and heat transmission rates while also potentially causing particle attrition [10].

**Pneumatic transport:** Pneumatic transport is the movement of solid particles through a pipeline utilizing a gas (typically air) as the transport medium. This approach is used to transport large quantities of materials over great distances in industries [10].

## 2.3 Particles classification

Fluidization of particles mostly depend on the size and density of the particles which was carefully investigated by Geldart and the following classification of four group of particle behavior was proposed by Geldart which is widely accepted and used to model fluidized bed [13].

- Group A: Small particles (30-150  $\mu\text{m}$ ) with low density ( $<1.4 \text{ g/cm}^3$ ). The fluidization is simple, smooth, and consistent. It permits operation with low gas flows while handling the growth and pace of the bubbles.
- Group B: Particles having a medium diameter (40-500  $\mu\text{m}$ ) and density of  $1.4\text{-}4 \text{ g/cm}^3$ . Fluidization is suitable for high gas flow rates. The bubbles tend to expand rapidly and occur at the start of fluidization.
- Group C: these are fine particles, under 30  $\mu\text{m}$  in size, hard to fluidized due to large interparticle forces. They cause channeling in small beds, for example talc, flour starch etc.
- Group D: known as ‘spoutable’ materials which are large, dense and hard to fluidized in deep beds. Higher velocity can create a jet, causing materials to be blown out in a spouting motion. Uneven gas distribution can lead to spouting behavior and several channeling. Examples: coffee beans, lead shot certain metal ores.

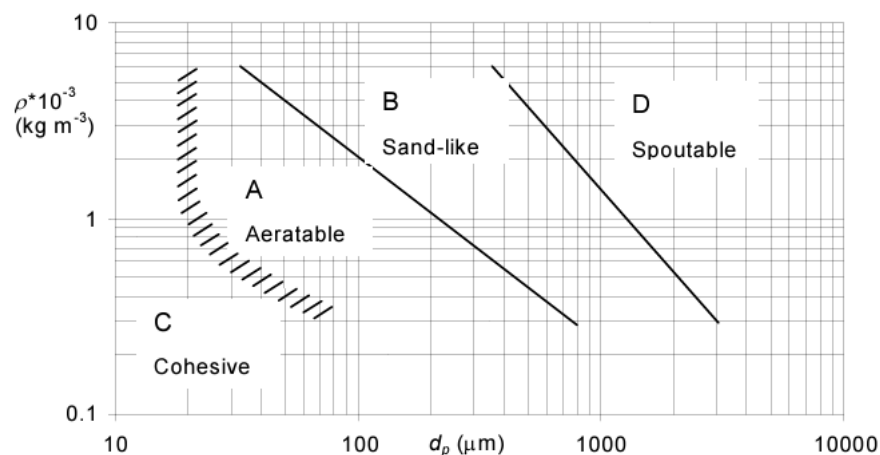


Figure 2.3: Classification of particles in 1973 by Geldart [13].

## 2.4 Particle size distribution

Particle size distribution (PSD) is a statistical representation of the sizes of particles in each sample. This method measures the relative proportions within specific size intervals, allowing for a better understanding of the physical attributes of the system. Comprehending and describing the particle size distribution (PSD) is essential for examining particulate materials in scientific and industrial environments. This allows for the investigation of several parameters such as the range of particle sizes, the average size, the width of the distribution, and the existence of agglomerates or aggregates.

Fluidized bed efficiency depends on parameters like material properties, mixture composition, gas velocity, solids flow rate, bed height, and geometrical parameters. Studying these factors can enhance fluidized bed system design and performance [11].

## 2.5 Bubbling fluidization bed

Bubbling fluidized bed is a dynamic system where solid particles are kept suspended and stirred by an upward flow of gas, usually air or another fluid. The gas velocity is regulated to ensure that the particles exhibit behavior like that of a boiling liquid, resulting in the formation of bubbles inside the bed. At operation this shows several regions along with its height. The following figure 2.4 shows the larger particles require comparatively more drag force to pull up so these particles form the dense phase in the bed, on the other hand smaller particles tends to fluidize easily and create lean phase or free board height [10].

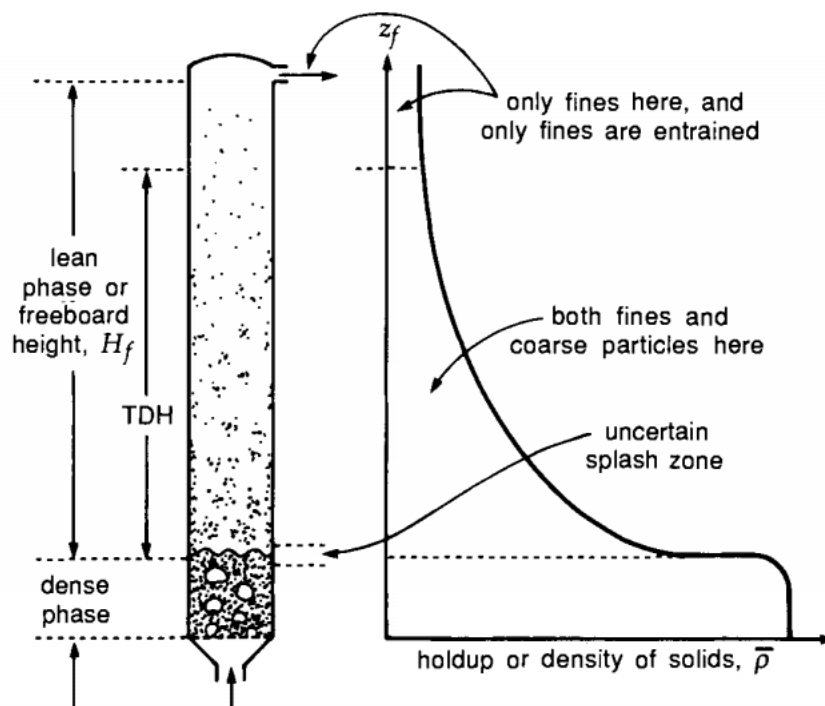


Figure 2.4: Dense phase and lean phase of particles in bubbling fluidized bed [10].

### 2.5.1 Lower zone

At the lower part of the bubbling fluidized bed as in figure 2.4, more particles stay close and comparatively the larger particles tend to be create more dense area. Bubbles appears here goes up and gain larger in bubble size finally reach top of particles. This area is known as dense phase [10].

### 2.5.2 Upper zone

The upper area of the bubbling fluidized bed contains less particles and most of them are comparatively smaller in size. These smaller particles need less drag force for lifting and goes up easily and create lean phase of the fluidized bed [10]. Figure 2.4 reveal that the fine particles are allowed to escape at the top, in the middle of the bed both coarse particles and fines particles are stay together. An uncertain splash area is also found in the bed where the particles are in transition between dense phase and lean phase.

## 2.6 Gas distributor design

Ceramic or sintered metal porous plate distributors are commonly employed in small-scale fluidization investigations due to their ability to offer high flow resistance, hence facilitating a uniform gas distribution across the bed. This is possible as well using alternative materials, such as filter cloth, compressed fibers, compacted wire plate, or a thin layer of microscopic particles. However, certain materials require reinforcement using metal or wire plates featuring substantial apertures. Although gas-solid contact is improved by these distributors, they possess certain limitations for industrial applications. Which are as follows [10]:

- high-pressure drop,
- low construction strength, high cost,
- low resistance to thermal stresses, and
- the possibility of blockage caused by tiny particles or corrosion by products.

Some common gas distributors listed with stoichiometric view are shown in figure 2.5, 2.6 and 2.7. Different gas distributors have different purpose and suitable to the process according to the nature of gas and the particles used in the bed as well as the bed parameters.

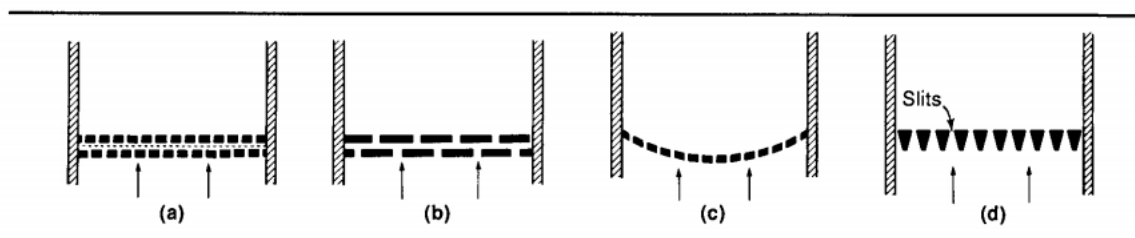


Figure 2.5: Gas distributors (a) sandwiching perforated plates;(b) staggered perforated plates; (c) dished perforated plate; (d) grate bars [10].

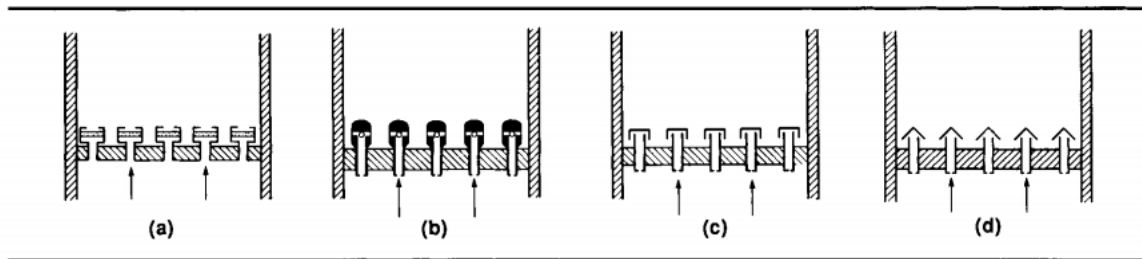


Figure 2.6: Gas distributors (a) porous plate types; (b) nozzle type (c) bubble Cap type still nozzle type [10].

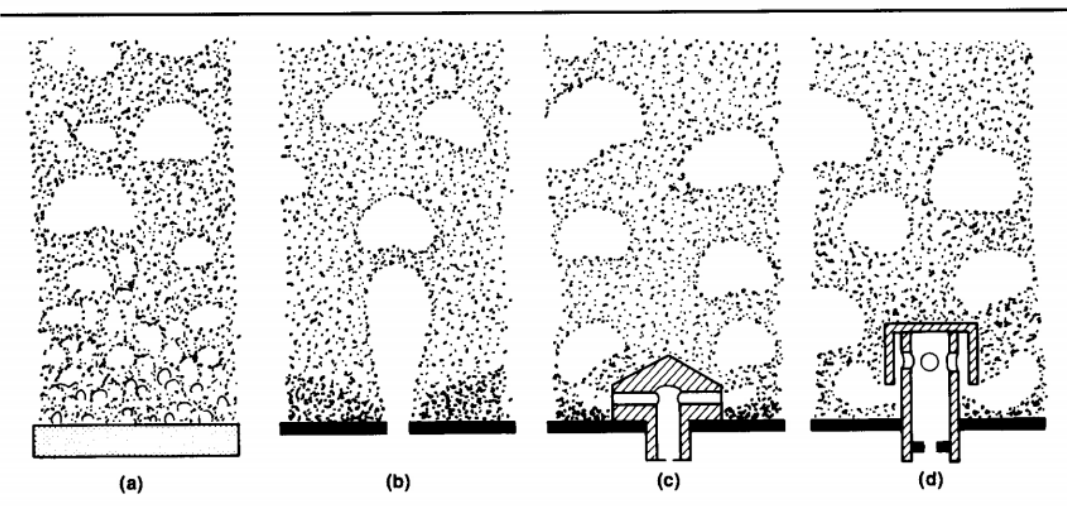


Figure 2.7: : Bubbles behaviors during fluidization (a) porous plate; (b) perforated plate; (c) nozzle-type tuyere; (d) bubble cap tuyere [10].

This study assumed a uniform gas distributor which has equal distribution of gas at the bottom of the cylindrical shape gas cooler.

Bubbling fluidized bed reactors achieve a yield of 70-75% in dry feed wood by maintaining a feed size of 2-3 mm to control heating rate and residence time of solids, the size of the reactor directly influences the rate at which it heats up. This reactor is special due to its utilization of fluidized flow of gases, which efficiently controls the residence rate of the solids and other substances [14].

Research on the transfer of heat to the walls of a fluidized bed has been conducted since 1949, particularly by Mickley and Trilling. Their study focused on a type of fluidized bed known as a circulating fluidized bed (CFB) [15]. The heat transfer coefficient directly affects the efficiency of a heat exchanger. Due to the complexity of fluidized bed phenomena, the influence of operational and geometric parameters on this coefficient is not always linear and can be difficult to identify. However, many studies have revealed some behaviors in heat transfer within fluidized beds [16].

The heat transfer coefficient is mostly influenced by the particle velocity and the particle volume fraction. As the velocity of the particles rises, the heat transfer coefficient also increases. This is because the agitation of the particles intensifies, leading to improved movement and exchange between the wall and the center of the tube [17].

## 2 Literature review

Brookhaven National Laboratory investigated the use of fluidized beds of granular particles in heat exchangers to prevent scale formation in high-temperature distillation of salty waters. By keeping the bed on the saltwater side, the tube surfaces remained scale-free even after prolonged testing with seawater at 330°F to 340°F. Calcium sulfate, forming as fresh feed was added, stayed in suspension, and did not accumulate on the bed particles or in the external piping system. The high heat transfer coefficients were maintained at around 850 Btu/hrft<sup>2</sup>°F [5].

The investigation of heat transfer in a bubbling fluidized bed with a submerged superheater tube bundles in a large-scale circulating fluidized bed boiler. The impact of bed particle size, suspension density, and fluidizing number on the heat transfer coefficient was studied. Parameters such as bubble fraction and emulsion contact time were calculated. A heat transfer model predicted varying heat transfer coefficients ranging from 255 to 381 W/(m<sup>2</sup>K), with smaller bed particle sizes leading to increased heat transfer. Additionally, longer emulsion contact times with tube surface decreased the average heat transfer coefficient [18]. On the other hand a numerical study on wall-to-bed heat transfer in a circulating fluidized bed (CFB) riser. 3-D CFD were conducted to analyze heat transfer characteristics. A heated portion (0.15 m x 0.60 m) was placed above the distributor plate. The wall of the heater maintained a constant heat flux of 1000 W/m<sup>2</sup>. The simulation considered air and sand mixture flow, using the RNG k-ε and Gidaspow models. For different Geldart B type particles sizes (60 μm to 460 μm) results found that the bed temperature and heat transfer coefficient increases with increasing bed inventory and particle size [19].

Temperature is almost constant throughout the bed in bubbling and turbulent fluidized bed. Bubbles in the fluidized bed cause upward and downward particle motion and the bubbles responsible for particle renewal at heat transfer surface. Vertical mixing is faster than lateral motion and contributes more to the bed performance [10]. A study aimed to develop engineering methods to predict heat transfer coefficient on tubes in bubbling fluidized beds. Heat transfer occurs through gaseous convection, particle convection/conduction, and radiation in high temperature operations. The recommended tube orientations are horizontal or vertical only [3].

A study on different materials has been conducted comparing stainless steel, aluminum, and copper as the particulate phase to observe the effect of particle properties such as the particle density, specific heat, thermal conductivity, and size on the heat transfer characteristics of a liquid–solid fluidized bed heat exchanger. The literature reveals that the final temperature (saturation temperature) sharply decreases in the fixed bed regime while the fluid velocity is rising. However, after minimum fluidization condition, there is no considerable difference between values of the saturation temperature at different liquid velocities. The particle density has two effects on the process: hydrodynamic and thermal. To isolate the hydrodynamic effects, the particle mass heat capacity was kept constant while changing the density. Increasing density resulted in a decrease in the final temperature value. Changing the specific heat capacity of particles does not significantly affect bed hydrodynamics and heat transfer, but it alters the energy absorption. The thermal conductivity of the stainless-steel particles has no major impact on saturation temperature values. Stainless steel particles have superior heat transfer rates compared to copper and aluminum. Particle diameter also affects heat transfer, with an optimum saturation temperature value at  $d_p \approx 2$  mm and a minimal  $Q_{max/saturation-temp}$  at the same diameter. This is due to changes in the particle's surface area and rising  $h$  value [20].

## 2 Literature review

Another study investigates heat transfer characteristics in a bubbling fluidized bed with a submerged superheated tube bundles in an integrated fluidized bed heat exchanger. The effects of bed particle size, suspension density, and fluidizing number on the average heat transfer coefficient were evaluated. The physical parameters of bed particles and fluidizing air were measured at different unit loads. Bubble fraction and contacting time of emulsion phase on the heat transfer surface were calculated. A heat transfer model was used to predict the coefficient, which varied from 255–381 W/(m<sup>2</sup>K), increasing with decreased particle size. Additionally, the coefficient decreased with increased contact time and for that solids mixing is reduced [18].



## 3 Theory

Some outcomes of theoretical study are described elaborately in this chapter which includes fluidization velocity, fluidized bed particles properties, CFPD, governing equations, thermal model as well as the thermal effect.

### 3.1.1 Minimum fluidization velocity

The minimum fluidized velocity ( $u_{mf}$ ) refers to the superficial velocity of the gas required for the initiation of fluidization in a packed bed. The state in consideration is called minimum fluidization or incipient fluidization, where the force of drag is equal to the net weight of a particle. The total drag force ( $F_D$ ) exerted on the bed can be calculated by multiplying the pressure drop ( $\Delta p_{mf}$ ) across the bed by its cross-sectional area (A) [13].

$$F = \Delta p_{mf} A \quad (3.1)$$

The net weight can be calculated as the product of bed volume ( $V_{mf} = AL_{mf}$ ), net density ( $\rho_s - \rho_f$ ) and the fraction ( $1 - \epsilon_{mf}$ ) of the bed occupied by the bed particles.

$$\Delta p_{mf} A = AL_{mf}(\rho_s - \rho_f)(1 - \epsilon_{mf})g \quad (3.2)$$

$$\frac{\Delta p_{mf}}{L_{mf}} = (\rho_s - \rho_f)(1 - \epsilon_{mf})g \quad (3.3)$$

Where  $\rho_s$  is particle density,  $\rho_f$  is fluid density,  $\epsilon_{mf}$  void fraction at minimum fluidization and  $g$  is the gravitational force. The density of fluidized solids is calculated by subtracting the fluid's density from the particles' density. The fraction of the bed that is occupied by particles is measured as the number of particles significantly contributes to the pressure drop.

The Ergun equation precisely calculates the minimum fluidization velocity (MFV) by evaluating the pressure drop per bed length using the following two terms [21].

$$\frac{d_p^3 \cdot \rho_f (\rho_s - \rho_f) g}{\mu^2} = \frac{1.75}{\epsilon_{mf}^3 \cdot \phi_s} \left( \frac{d_p \cdot u_{mf} \cdot \rho_f}{\mu} \right)^2 + \frac{150(1 - \epsilon_{mf})}{\epsilon_{mf}^3 \cdot \phi_s^2} \left( \frac{d_p \cdot u_{mf} \cdot \rho_f}{\mu} \right) \quad (3.4)$$

Or,

$$Ar = \frac{1.75}{\epsilon_{mf}^3 \cdot \phi_s} (Re_{mf})^2 + \frac{150(1 - \epsilon_{mf})}{\epsilon_{mf}^3 \cdot \phi_s^2} (Re_{mf}) \quad (3.5)$$

Where,  $Ar$  is Archimedes number,  $\phi_s$  is particle sphericity.

$$Ar = \frac{d_p^3 \cdot \rho_f (\rho_s - \rho_f) g}{\mu^2} \quad (3.6)$$

And Reynold's number at minimum fluidization velocity is.

$$Re_{m_f} = \frac{d_p \cdot u_{m_f} \cdot \rho_f}{\mu} \quad (3.7)$$

The minimum fluidized velocity is as follows:

$$u_{m_f} = \frac{d_p^2 (\rho_s - \rho_f) g}{150 \mu} \cdot \frac{\varepsilon_{m_f}^3 \cdot \phi_s^2}{1 - \varepsilon_{m_f}} \quad (3.8)$$

### 3.1.2 Minimum bubbling velocity

The superficial velocity at which the first bubble appears in fluidization is denoted as minimum bubbling velocity. Abrahamson And Geldart (1980) proposed a ratio  $\left(\frac{u_{mb}}{u_{m_f}}\right)$ , which indicate the degree at which bed expansion occurs and the ration particularly depends on the fraction of fines particles below 45 $\mu\text{m}$  [22].

$$\frac{u_{mb}}{u_{m_f}} = \frac{2300 \rho_f^{0.13} \mu^{0.52} \exp(0.72F)}{d_p^{0.8} g^{0.934} (\rho_s - \rho_f)^{0.93}} \quad (3.9)$$

Where,  $u_{mb}$  is the minimum bubbling velocity,  $u_{m_f}$  is the minimum fluidization velocity,  $\rho_f$  is the density of fluid,  $d_p$  is average particle diameter,  $\rho_f$  is density of fluid,  $P_{45}$  is particle weight fraction < 45  $\mu\text{m}$ .

### 3.1.3 Terminal velocity

Terminal velocity in a fluidized bed is the highest velocity at which particles can settle in the fluidized condition. It occurs when the upward drag force on the particles is equal to the downward force of gravity. This can be estimate by the following equation [23].

$$u_t = u_t^* \left[ \frac{\mu (\rho_s - \rho_f) g}{\rho_f^2} \right]^{\frac{1}{3}} \quad (3.10)$$

The dimension less terms  $u_t^*$  of the above equation are calculated as by following equations.

$$u_t^* = \left[ \frac{18}{(d_p^*)^2} + \frac{2.335 - 1.744 \cdot \phi_s}{(d_p^*)^{0.5}} \right]^{-1} \quad (3.11)$$

Where the range of the particle sphericity is  $0.5 < \phi_s < 1$  and dimensionless particle size  $d_p^*$  is calculated by the following equation.

$$d_p^* = d_p \left[ \frac{\rho_f \cdot (\rho_s - \rho_f) g}{\mu^2} \right]^{\frac{1}{3}} \quad (3.12)$$

### 3.1.4 Mean diameter

Mean diameters ( $d_p$ ) reveal the average diameter of the particles parent in the range of particle size distribution, and it is calculated as 70  $\mu\text{m}$  (appendix A).

### 3.1.5 Other particle properties

The hydrodynamics of a fluidized bed is very critical and tough to predict as this is dependable on various factors. Particles properties dominate most of the state of hydrodynamics of fluidized bed. Particle Sphericity, Void Fraction, Skeletal density, true density, bulk density, envelop density etc. have important effects on fluidization of particles.

**Particle Sphericity:** Sphericity measures how closely a particle resembles a sphere by comparing surface areas. It is defined as  $\Phi_s$  and this can be express as follows.

$$\Phi_s = \left( \frac{\text{surface of sphere}}{\text{surface of particles}} \right)_{\text{of same volume}} \quad (3.13)$$

According to the definition the sphericity of sphere is 1 and for other particles the range is  $0 < \Phi_s < 1$  [10]. For this study the particle sphericity of alumina is considered as 0.7 in appendix E.

**Void Fraction:** Void Fraction ( $\theta_{cp}$ ) measures empty spaces in powder, range of void fraction express as in between 0 and 1. Void fraction at minimum fluidization is taken as 0.442 for this study, appendix E.

**Bulk density:** Bulk density is simply the mass of material per unit volume. However, for powders, bulk density is not reliable as it can vary greatly based on packing. Additionally, powders' bulk density can change over time [24].

**True density:** True particle density is an inherent property of material, unaffected by size, shape, compaction, or packing, and remains constant and this is not change over time [24].

**Envelop density:** The ratio of particle mass to the combined volumes of solid and voids within each piece is refers to the ratio of particle mass to the envelope volume according to (ASTM D3766) [25]. Envelop density is considered for alumina as 1900  $\text{kg/m}^3$  in this study, appendix E.

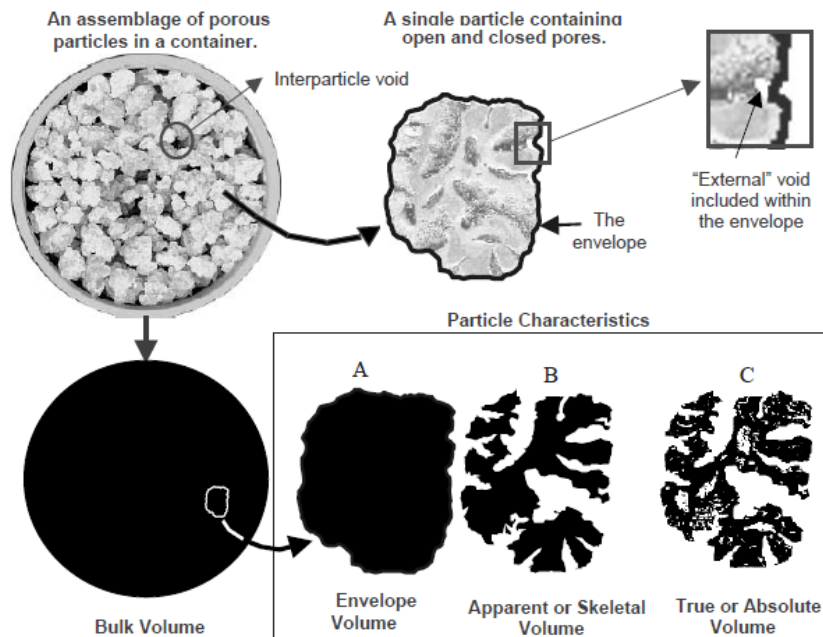


Figure 3.1: Various particle properties [24].

## 3.2 Grid generation

Gridding, or meshing, is crucial for computational fluid dynamics simulation. It determines simulation time and precision. Poor mesh quality leads to inaccurate results. Expertise in grid generation is as important as other steps in the simulation process, which typically has five main steps [26].

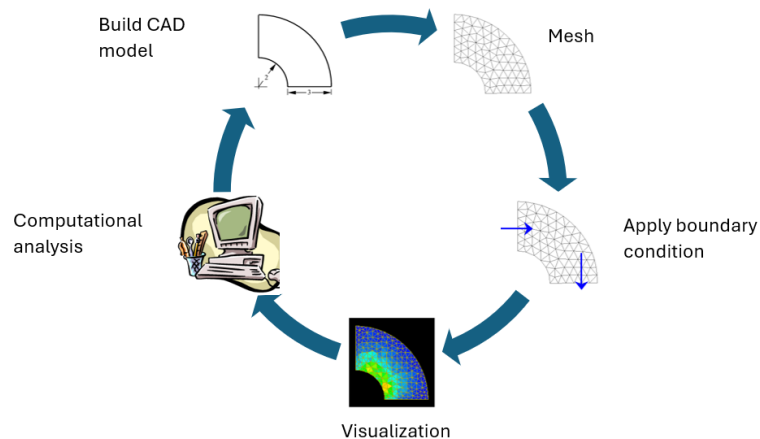


Figure 3.2: Steps of gridding, meshing and analysis in CPFD [26].

### 3.3 CPF D terminology

A mesh is a technique that divides a geometry into several components for calculation. The CPF D solver utilizes these elements to create control volumes. The diagram illustrates the key components to describe the terms [26].

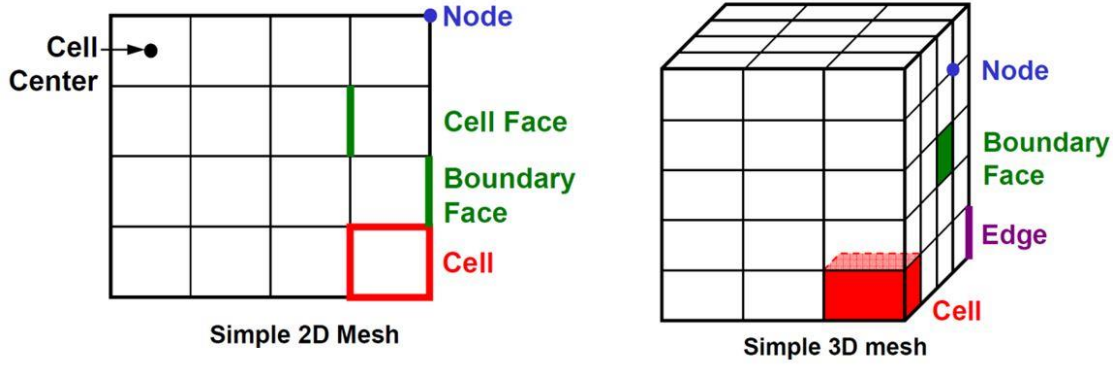


Figure 3.3: 2D and 3D mesh in CPF D [26].

The above figure 3.3 shows the 2D and 3D mesh, and its various terms used in CPF D simulation. The nomenclature of these components is defined as follows,

- Cell = control volume into which domain is broken up.
- Node = grid point.
- Cell center = center of a cell.
- Edge = boundary of a face.
- Face = boundary of a cell.
- Zone = grouping of nodes, faces, cells
- Domain = group of node, face, and cell zones.

### 3.4 Governing equation

Continuous and Particulate Phase are two approaches to for a fluid with no interphase mass transfer which is [27]:

$$\frac{\partial \theta_f}{\partial t} + \nabla \cdot (\theta_f \cdot u_f) = 0 \quad (3.14)$$

Where  $u_f$  is the fluid velocity and  $\theta_f$  is the fluid volume fraction. Then the momentum equation for the fluid is

$$\frac{\partial (\theta_f u_f)}{\partial t} + \nabla \cdot (\theta_f u_f u_f) = -\frac{1}{\rho_f} \nabla_p - \frac{1}{\rho_t} \cdot F + \theta_f g \quad (3.15)$$

The rate of momentum exchange per volume between the fluid and particle phases, both of which are isothermal and incompressible, is denoted as F. The momentum equation discussed here does not consider viscous molecular diffusion within the fluid. However, the interphase drag power, F, accounts for the viscous drag between particles and fluid. While ignoring the

laminar fluid viscous terms has minimal impact on dense particle flow, these terms can be easily added to the fluid equation set. Unfortunately, there are currently no appropriate models for dense particle flow, particularly for turbulent flow. Gas movement around closely packed particles generates small sub-grid eddies and dissipation, while high-density particles act as larger eddies for momentum transfer. Additionally, particles adhering to walls with sizes like or larger than the viscous sublayer complicate momentum transfer at walls. The turbulent dense particle flow is not addressed in this equation. However, the transfer of momentum from discrete particles to the fluid, achieved through a turbulent closure model for sub-grid momentum transfer, effectively predicts dense particle flows across a wide range of gas flow conditions[27].

The particle probability distribution function  $\phi(X, u_p, \rho_p, \Omega_p, t)$  in the Particulate Phase defines the dynamics of particle position, velocity, density, and volume. Mass remains stable but size and density may vary. Solving the Liouville equation gives the evolution of  $\phi$ .

$$\frac{\partial \phi}{\partial t} + \nabla \cdot (\phi \mathbf{u}_p) + \nabla_{u_p} \cdot (\phi A) = 0 \quad (3.16)$$

Where  $\nabla_u$  is the divergence operator with respect to velocity. According to the definition[28], the discrete particle acceleration,  $A$ , can be defined as

$$A = D_p(\mathbf{u}_f - \mathbf{u}_p) - \left( \frac{1}{\rho_p} \nabla p + \frac{1}{\theta_p \rho_p} \cdot \tau \right) + g \quad (3.17)$$

Acceleration terms include aerodynamic drag, pressure gradient, interparticle stress gradient, and gravity. Probability function gives particle count per unit volume at specific time intervals  $(u_p, u_p + du_p)$ ,  $(\rho_p, \rho_p + d\rho_p)$ , and  $(\Omega_p, \Omega_p + d\Omega_p)$ . Particle volume fraction is calculated using the distribution function refers as follows.

$$\theta_p = \int \int \int \phi \Omega_p d\Omega_p d\rho_p d\mathbf{u}_p \quad (3.18)$$

The interphase momentum transfer function per volume in the Eulerian momentum equation is:

$$F = \int \int \int \phi \Omega_p \rho_p \left[ D_p(\mathbf{u}_f - \mathbf{u}_p) - \frac{1}{\rho_p} \nabla p \right] d\Omega_p d\rho_p d\mathbf{u}_p \quad (3.19)$$

The Eulerian governing equations for the particle phase may be obtained by taking the moments of (4.3) and the particle conservation equations are found by multiplying equation number (4.3) by  $\Omega_p \rho_p$  and  $\Omega_p \rho_p \mathbf{u}_p$  and integrating across particle density, volume, and velocity coordinates. The particle equation is:

$$\frac{\partial (\overline{\theta_p \cdot \rho_p})}{\partial t} + \nabla \cdot (\overline{\theta_p \rho_p \mathbf{u}_p}) = 0 \quad (3.20)$$

And the particle momentum equation is:

$$\begin{aligned}
\frac{\partial(\overline{\theta_p \cdot \rho_p})}{\partial t} + \nabla \cdot (\overline{\theta_p \rho_p \mathbf{u}_p \mathbf{u}_p}) \\
= -\theta_p \nabla p - \nabla \tau_p + \overline{\theta_p \rho_p} g + \int \int \int \phi \Omega_p \rho_p [D_p(\mathbf{u}_f - \mathbf{u}_p)] d\Omega_p d\rho_p d\mathbf{u}_p \\
- \nabla \cdot [\int \int \int \phi \Omega_p \rho_p [(\mathbf{u}_p - \overline{\mathbf{u}_p})(\mathbf{u}_p - \overline{\mathbf{u}_p})] d\Omega_p \cdot d\rho_p \cdot d\mathbf{u}_p]
\end{aligned} \tag{3.21}$$

Where the mean particle velocity  $\overline{\mathbf{u}_p}$  is given by

$$\overline{\mathbf{u}_p} = \frac{1}{\overline{\theta_p \rho_p}} \int \int \int \phi \Omega_p \rho_p \mathbf{u}_p d\Omega_p d\rho_p d\mathbf{u}_p \tag{3.22}$$

The average density is given by

$$\overline{\theta_p \rho_p} = \int \int \int \phi \Omega_p \rho_p d\Omega_p d\rho_p d\mathbf{u}_p \tag{3.23}$$

Where the volume fraction of fluid and particle phase must one,  $\theta_f + \theta_p = 1$ .

### 3.5 Thermal modeling in CPFDD

Several types of heat transfer mechanisms are considered in the fluidized bed in which convective fluid to wall heat transfer, convective fluid to particle heat transfer and radiation heat transfer are most dominating mechanisms [29].

**Isothermal:** An isothermal model assumes a constant temperature throughout the system and does not solve heat transfer equations. This allows for faster simulation. In Barracuda Virtual Reactor, the default isothermal temperature is 300 K.

**Non-isothermal:** A thermal model, on the other hand, calculates temperature gradients and considers factors such as boundary conditions, thermal walls, and chemical reactions.

Appropriate areas must specify thermal properties, heat transfer coefficients, initial fluid and particle temperatures, and boundary condition temperatures [29].

#### 3.5.1 Convective fluid to wall heat transfer mechanism

The local heat transfer coefficient at the fluid-wall interface,  $h_{fw}$ , is determined by the combined effects of the heat transfer coefficients in the lean gas phase,  $h_l$ , and the dense particle phase,  $h_d$ . The heat transfer coefficient between the fluid and the wall is multiplied by the function  $f_d$ , which represents the proportion of time that the dense particle phase is in contact with the wall. The time fraction of dense phase contact,  $f_d$ , depends on the particle volume fraction at the wall,  $\theta_p$ , and the close pack value fraction,  $\theta_{cp}$  [29].

$$h_{fw} = h_l + f_d h_d \tag{3.24}$$

$$f_d = 1 - e^{-10(\theta_p/\theta_{cp})} \tag{3.25}$$

**Lean phase:** For lean phase heat transfer coefficient, the general form can be express as follows [29].

$$h_l = ((c_0 Re_L^{n_1} Pr^{n_2} + c_1) \frac{k_f}{L} + c_2) \quad (3.26)$$

Where  $n_1, n_2, c_0, c_1, c_2$  are adjustable model parameters, the thermal conductivity of the fluid is denoted as  $k_f$ , while the cell length is represented by  $L$ . The Reynolds number and Prandtl number are specifically specified as

$$Re_L = \frac{\rho_f \cdot U_f \cdot L}{\mu_f}, \quad Pr = \frac{\mu_f \cdot c_{pf}}{k_f} \quad (3.27)$$

Where  $\rho_f$  is the fluid density,  $U_f$  is the fluid velocity,  $\mu_f$  is the fluid viscosity and  $c_{pf}$  is the fluid heat capacity. This correlation is based on Douglas and Churchill, [30]. Where  $n_1 = 0.5$ ,  $n_2 = 0.33$ ,  $c_0 = 0.46$ ,  $c_1 = 3.66$ ,  $c_2 = 0.0$

**Dense phase:** For the dense phase the general expression for the heat transfer coefficient is as follows [29].

$$h_d = (c_0 Re_p^{n_1} \frac{k_f}{d_p}) \quad (3.28)$$

The Reynolds number and Prandtl number are specified as

$$Re_p = \frac{\rho_f \cdot U_f \cdot d_p}{\mu_f} \quad (3.29)$$

Here  $n_1 = 0.75$ ,  $c_0 = 0.525$ .

### 3.5.2 Convective fluid to particle heat transfer mechanism

The transfer of heat between the fluid phase and the particle phase is represented by the fluid-to-particle heat transfer coefficient. The fluid-to-particle heat transfer coefficient can be expressed as follows [29].

$$h_p = ((c_0 Re_L^{n_1} Pr^{0.33} + c_1) \frac{k_f}{L} + c_2) \quad (3.30)$$

Where  $n_1, c_0, c_1, c_2$  are adjustable model parameters, the thermal conductivity of the fluid is denoted as  $k_f$ . The Reynolds number specified as

$$Re_p = \frac{\rho_f \cdot (U_f - U_p) \cdot d_p}{\mu_f}, \quad Pr = \frac{\mu_f \cdot c_{pf}}{k_f} \quad (3.30)$$

The variables in the equation are defined as follows:  $\rho_f$  represents the density of the fluid,  $U_f$  represents the velocity of the fluid,  $U_p$  represents the velocity of the particle,  $\mu_f$  represents the viscosity of the fluid, and  $c_{pf}$  represents the heat capacity of the fluid.

The Nusselt number is lower in fluidized beds compared to a single sphere when the Reynolds number is below 20. In a fluidized bed, the bubbling phenomenon causes the Nusselt number



to be lower than 2.0. This is due to the presence of entrained particles in low Reynolds number beds, which reduces the efficiency of particle-gas contact. However, in beds with larger particle diameters, gas-particle contact improves. To capture fluid-to-particle heat transfer in a fluidized bed, Virtual-Reactor uses a correlation based on McAdams' 1954 proposal [31] and the model parameters are  $n_1 = 0.6$ ,  $c_0 = 0.37$ ,  $c_1 = 0.01$ ,  $c_2 = 0.0$ .

This correlation corresponds with the experimental evidence of Turton and Levenspiel on the heat transfer coefficient between particles and fluid in fluidized beds with small particles [10].

### 3.5.3 Radiation thermal flow

The P-1 radiation model considers thermal radiation interactions between particles, between particles and fluids, between particles and thermal barriers, and between fluids and thermal walls. This model can be utilized with or without Thermal Wall Boundary Conditions (BCs) [29].

The transport equation for the incident radiation in the P-1 radiation model is as follows

$$\nabla \cdot (\Gamma \nabla G) + 4(an^2\sigma T^4 + E_p) - (a - a_p)G = 0 \quad (3.31)$$

By specifying any Thermal Wall Boundary Conditions (BCs), the Marshak boundary condition is applied to determine the radiative heat flux at the thermal wall,  $q_w$ :

$$-q_w = T_w \left( \frac{\partial G}{\partial n} \right) = \frac{\varepsilon_w}{2(2 - \varepsilon_w)} \cdot (4\sigma T_w^4 - G_w) \quad (3.32)$$

Where,

$\Gamma$  is radiation diffuse coefficient in units of  $m$

$G$  is incident radiation to be solved in units of  $J/s/m^2$

$a$  is absorption coefficient of the fluid mixture in units of  $1/m$

$n$  is refractive index of the fluid mixture

$\sigma$  is the Stefan-Boltzmann constant.

$T$  is fluid temperature in units of  $K$

$E_p$  is equivalent emission of the particles

$a_p$  is equivalent particle absorption coefficient in units of  $1/m$

$\varepsilon_w$  is the emissivity of the thermal wall

The radiation diffuse coefficient is defined as the following equation,

$$\Gamma = \frac{1}{3(a + a_p + \sigma_f + \sigma_p)} \quad (3.33)$$

The mixing rule is used to calculate the average qualities of a fluid mixture based on its components.

$$a = \sum_{i=1}^{n_f} y_{f_i} \cdot a_{f_i} \quad (3.34)$$

The equivalent particle absorption coefficient is:

$$a_p = \sum_{i=1}^{n_p} \frac{A_{pi}}{V} \cdot \epsilon_{f_i} \quad (3.35)$$

The equivalent fluid scattering coefficient is:

$$\sigma_p = \sum_{i=1}^{n_f} y_{f_i} \cdot \sigma_{f_i} \quad (3.36)$$

Where  $\sigma_{f_i}$  is scattering coefficient of fluid.

The equivalent particle scattering factor is:

$$\sigma_p = \sum_{i=1}^{n_p} \frac{A_{pi}}{V} \cdot (1 - \epsilon_{f_i}) \cdot (1 - \sigma_{f_i}) \quad (3.37)$$

The refractive index of the fluid mixture, is calculated as:

$$\frac{n^2 - 1}{n^2 + 2} = \sum_{i=1}^{n_f} x_{f_i} \frac{n_{f_i}^2 - 1}{n_{f_i}^2 + 2} \quad (3.38)$$

The heat source, or sink, due to radiation,  $q_r$  is:

$$-\nabla \cdot q_p = \nabla \cdot (\Gamma \nabla G) = (a + a_p)G - 4(an^2\sigma T^4 + E_\rho) \quad (3.39)$$

Radiation is accounted for in the fluid and particle energy equations by incorporating the heat source into them [29].

### 3.5.4 Available model for drag force and drag model selection

In Barracuda VR®, the drag model calculates the force exerted on a particle ( $F_p$ ), by the model's fluid. Virtual Reactor included various drag model fits for its specific features and can use the drag models mentioned below [32].

- Constant Drag
- Stokes
- Wen-Yu
- Ergun
- WenYu-Ergun
- Turton-Levenspiel
- Richardson, Davidson, and Harrison
- Haider-Levenspiel
- EMMS-Yang-2004
- Non-spherical Ganser
- Non-spherical Haider-Levenspiel

Drag models calculate force ( $F_p$ ), on a particle based on fluid and particle properties and flow conditions, including mass ( $m_s$ ), fluid velocity ( $u_f$ ), particles velocity ( $u_s$ ), and drag function ( $\hat{D}$ ). The force is calculated by following equation [32].

$$F_p = m_s D(u_f - u_s) \quad (3.40)$$

**WenYu-Ergun drag model:** Fluidized bed system contains both dilute phase as well as dense phase, according to Bandara et al. [33] WenYu-Ergun drag model fits the best for the system.

For the dilute system, the Wen-Yu drag model is used and is expressed as:

$$D_1 = \frac{3}{8} C_d \frac{\rho_f |u_f - u_s|}{r_s \rho_s} \quad (3.41)$$

Here  $C_d$  is the drag coefficient and given as a function of the Reynolds number.

$$\begin{aligned} C_d &= \frac{24}{Re} \theta_f^{-2.65} & Re < 0.5 \\ C_d &= \frac{24}{Re} \theta_f^{-2.65} (1 + 0.15 Re^{0.687}) & 0.5 \leq Re \leq 1000 \\ C_d &= 0.44 \theta_f^{-2.65} & Re > 1000 \end{aligned} \quad (3.42)$$

Where Reynolds ( $Re$ ) number is calculated by

$$Re = \frac{2\rho_f r_s (u_f - u_s)}{\mu_f} \quad (3.43)$$

$r_s, \mu_f$  is the particle radius and fluid viscosity.

For the dense system, the Ergun drag model is considered,

$$D_2 = 0.5 \left( \frac{180\theta_s}{\theta_s Re} + 2 \right) \frac{\rho_f |u_f - u_s|}{r_s \rho_s} \quad (3.44)$$

The blended Wen-Yu/Ergun drag model can be expressed as:

$$D = \begin{cases} D_1 & \theta_s < 0.75\theta_{CP} \\ (D_2 - D_1) \left( \frac{\theta_s - 0.75\theta_{CP}}{0.85\theta_{CP} - 0.75\theta_{CP}} \right) & 0.75\theta_{CP} \geq \theta_s \geq 0.85\theta_{CP} \\ D_2 & \theta_s > 0.85\theta_{CP} \end{cases} \quad (3.45)$$

WenYu-Ergun drag model is used for multiphase flow simulations, particularly for gas-solid fluidized system. This drag model is chosen for the simulation as the particles of the bed contain both dilute phase as well as the dense phase of particles. This combined drag model effectively handle the flow regimes, ranging from dilute phase to dense phase. The WenYu part of the model applied for the dilute phase where particle to particle interaction is nominal and the Ergun part of the model deals with dense phase where the particle-to-particle interactions are significant.

## 4 Methodology

Fluidized bed used as a heat exchanger like gas cooler, need to be shaped considering several factors related to the geometry of the gas cooler as well as the parameters which have direct effect for heat transfer requires calculation to obtain optimum value fits for the system. Following stepwise approaches are being considered as the core method to find the best.

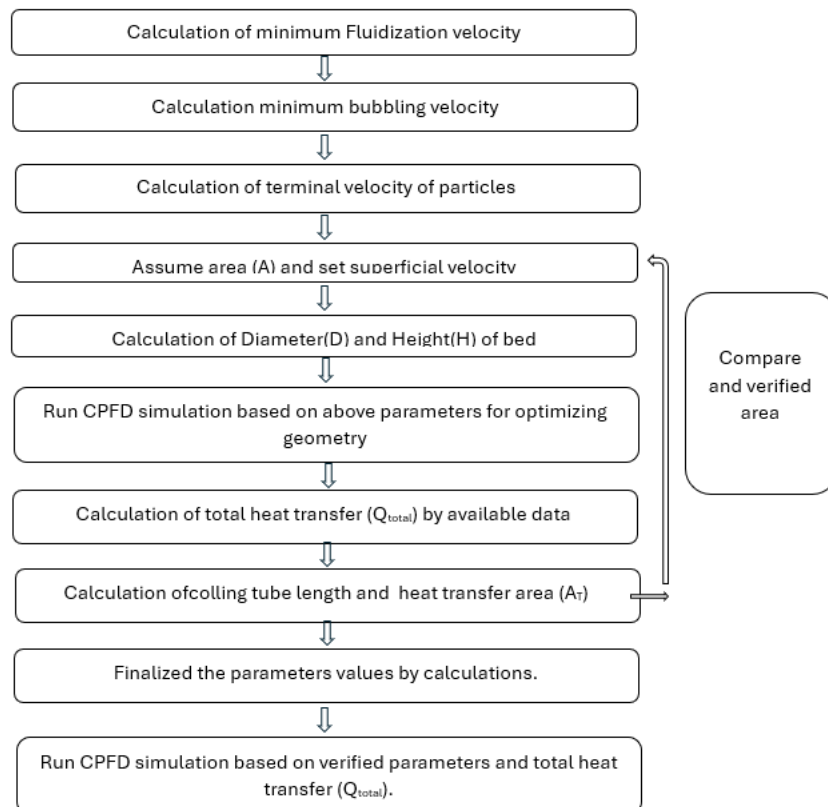


Figure 4.1: Overview of methodology.

The above figure 4.1 is the summary of the consecutive steps followed in this study. Firstly, the minimum fluidization velocity ( $u_{mf}$ ), minimum bubbling velocity ( $u_{mb}$ ) and terminal velocity ( $u_t$ ) is calculated to obtain the range ( $u_{mf} < u_{mb} < u_{sf} < u_t$ ) of superficial velocity ( $u_{sf}$ ) which provide better fluidization. The fluidized bed height, diameter, total particle mass in the bed is calculated to get geometry of the bed. Secondly, the thermal calculation is being carried out to obtain the heat transfer surface area, tube length, coolant flowrate as well as the overall cooling load.

### 4.1 Thermal approach

Conduction, convection, and radiation are three ways to transfer thermal energy. Conduction occurs through temperature gradients, measured by heat conductivity. Convection occurs when heat is carried by fluid movement, either forced or natural. Radiation happens when energy is transferred between surfaces with different temperatures through electromagnetic waves.

Radiation is significant at high temperatures, including combustion, but can also impact room temperatures [34].

## 4.2 Cooling load

Heat transfer takes place between the fluidized particle/gas medium, known as the 'bed', and the submerged tube surfaces, known as the 'walls'. The overall heat transfer ( $Q_{overall}$ ) from bed materials to tube surfaces is assumed as equal according to energy conservation law [35].

$$Q_{overall} = Q_{walls} = Q_{bed} \quad (4.1)$$

Assuming the total available energy in the bed are obtained from the inlet carbon di oxide gas which targeted to cool down by releasing thermal energy at the surface of tubes. Total heat contain in a stream of a gas is being determined by following equation.

$$Q_{bed} = Q_{CO_2} = \dot{m}_{CO_2} \cdot C_{p,CO_2} (T_{hot,in} - T_{hot,out}) \quad (4.2)$$

Where  $\dot{m}_{CO_2}$  is the flow rate of hot gas enter to the bed,  $C_{p,CO_2}$  heat capacity of the gas at considered temperature,  $T_{hot,in}$  is the inlet temperature and  $T_{hot,out}$  is the possible outlet temperature of gas. Similarly, the available thermal energy is transferred to the tubes contain the coolant, water in this case, also being determined as follows:

$$Q_{wall} = Q_{water} = \dot{m}_{water} \cdot C_{p,water} (T_{cold,in} - T_{cold,out}) \quad (4.3)$$

Where  $\dot{m}_{water}$  is the flow rate of hot coolant enter to the tubes,  $C_{p,water}$  heat capacity of the water at considered temperature,  $T_{hot,in}$  is the inlet temperature and  $T_{hot,out}$  is the possible outlet temperature of water as coolant.

As the said earlier of this section the total thermal energy of bed materials is the maximum heat available for the coolant to the taken out, so above equation can be combined to have follows:

$$\dot{m}_{water} = \frac{Q_{water}}{C_{p,water} (T_{cold,in} - T_{cold,out})} \quad (4.4)$$

Assuming the flow of two stream of the hot gas and the coolant in the fluidized bed as crossflow, Number of Transfer Units (NTU) method for heat exchanger calculation is considered. NTU is a dimensionless number which is widely used for heat exchanger analysis defined as [36].

$$NTU = f\left(\varepsilon, \frac{C_{min}}{C_{max}}\right) \quad (4.5)$$

Where  $\varepsilon$  is the effectiveness of heat exchanger. The effectiveness  $\varepsilon$  of the heat exchanger can be determined as follows.

$$\varepsilon = \frac{Q}{Q_{max}} \quad (4.6)$$

Where  $Q_{max}$  is the maximum heat transfer possible and formulated as,

$$Q_{max} = C_{min}(T_{hot,in} - T_{cold,in}) \quad (4.7)$$

Where  $C_{min}$  is equal to  $C_{cold}$  or  $C_{hot}$ , which ever is smaller.  $C_{cold}$  and  $C_{hot}$  is calculated according to following equations.

$$C_{cold} = \dot{m}_{water} C_{p,water} \quad (4.8)$$

$$C_{hot} = \dot{m}_{CO_2} C_{p,CO_2} \quad (4.9)$$

The ration of  $\frac{C_{min}}{C_{max}}$  is calculated and NTU also be calculated with the help of empirical correlation in between. The area of the heat transfer surface is then calculated by following equation.

$$NTU = \frac{h \cdot A_{tube}}{C_{min}}, \quad A_{tube} = \frac{NTU \cdot C_{min}}{h} \quad (4.10)$$

Where  $h$  is overall heat transfer coefficient  $W/m^2.K$ ,  $A_{tube}$  is the overall surface area of the cooling tubes. The internal cooling tubes is considered as uniform cylindrical tubes, and the surface area is equal to the heat transfer area calculated earlier.

$$A_{tube} = 2\pi r l \quad (4.11)$$

Or,

$$l = \frac{A_{tube}}{2\pi r} \quad (4.12)$$

Where,  $l$  is the total length of the cooling tubes,  $r$  is the radius of the cooling tubes.

### 4.3 Fluidized bed approach

Fluid hydrodynamics and performances of a fluidized bed largely depend on the geometrical parameters of fluidization bed. This method has studied to find out the best parameters at which the particles will be fluidized in maximum efficiency in a bubbling fluidized bed condition as well as least particles out flow. Several cases have been performed in simulation for different superficial velocities ( $0.05 \text{ m/s}^2$ ,  $0.07 \text{ m/s}^2$ ,  $0.09 \text{ m/s}^2$ ,  $0.11 \text{ m/s}^2$ ,  $0.13 \text{ m/s}^2$ ), different H/D ratio (0.5, 1.0, 1.5, 2.0, 2.5) and various area.

**Finding optimum H/D ratio:** The diameter of the cylindrical bed is calculated initially, and the superficial velocity is set as  $0.09 \text{ m/s}^2$  and several simulations done in the CFPD software at which the particle entrainments is observed. This output confirms the optimum height to bed ratio.

**Finding optimum superficial velocity:** the optimum H/D ratio and constant diameter as like previous are simulated with various superficial velocity which provide an optimum superficial velocity in which the fluidized bed performs efficiently which minimum particle out flow.

**Finding Optimum Area/diameter:** several simulations help to find out the area optimum with previously obtained H/D ratio and superficial velocity. This area of the cylindrical fluidized bed is considered as the best to install the cooling system into the fluidized bed.

#### 4.4 Thermal flow consideration

The total heat transfer, the heat transfer surface area, the tube length as well as the total coolant load in the fluidized bed has been calculated. To observe the performance of heat transfer efficiency of the bubbling fluidized bed of given data and calculated others geometrical parameters horizontal tube alignment and vertical tube alignment is considered for further analysis.

**Heat load:** Heat load of the fluidized bed shown negative value as the system perform as cooler. For simplicity the flow is considered as the crossflow system and the overall heat transfer is calculated according to the equation (4.2) in section three.

**Tube length & coolant flow rate:** Heat transfer surface area is calculated according to the equation (4.11), which then give the tube length having same surface area for heat transfer. The available water at 30°C is used as coolant and the required coolant flowrate is also calculated by using the equation no (4.4).

**Horizontal tubes:** Assuming the outlet coolant temperature of different values, five different cases has been performed in the simulation and best heat transfer efficiency is noted.

**Vertical tubes:** Similar analysis also contacted on the vertical tubes alignment which reveal the heat transfer efficiency of the fluidized bed and then compare to each other.

#### 4.5 Internal cooling tube design

To study the heat transfer effect on the bed, two types of cooling tube arrangement is considered. Fluidized bed hydrodynamics and the particle collision to tube surface and walls has significant impact on the heat transfer. These two alignments allow particles different ways to come contact and time of contact is also important. Computational Particle Fluid Dynamics (CPFD) Barracuda VR<sup>®</sup> software version 23.1.0 is used for simulation of several cases. The Barracuda Virtual Reactor is an engineering tool used for simulating and optimizing particle-fluid systems. Successful model setups can be used for various simulations with minor modifications. It is crucial to understand the required output data, data analysis, and potential future modifications when setting up a model. In Barracuda, simulation and post-processing parameters should be established for accurate calculations and helpful data reporting. This section provides a concise introduction to simulation parameters and the step-by-step process for defining a model.

**Vertical tube:** Three coil of vertical tubes are inserted in the dense phase of the particles. Equal distance is maintained among the tubes so that the particles have enough space for entrainment. The tube length and diameter of the tubes are calculated based on the parameters involved in the interaction. Following figure 4.2 shows a simple arrangement vertical cooling tube in the bed.



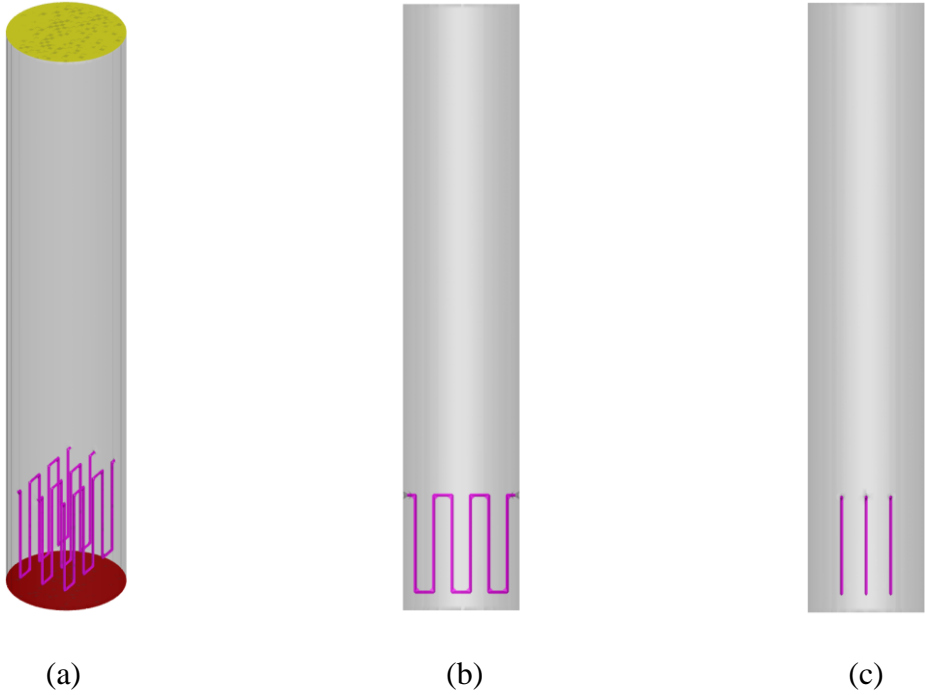


Figure 4.2: Vertical cooling tubes alignment (a) x-y-z view, (b) x-z plan, (c) x-z plan.

**Horizontal tube:** Horizontal cooling tubes figure 4.3 are also considered to observe the heat transfer effect on the bed. The tubes length and diameter of the tubes are also calculated as previous. Several cases are run in the simulation for these arrangements.

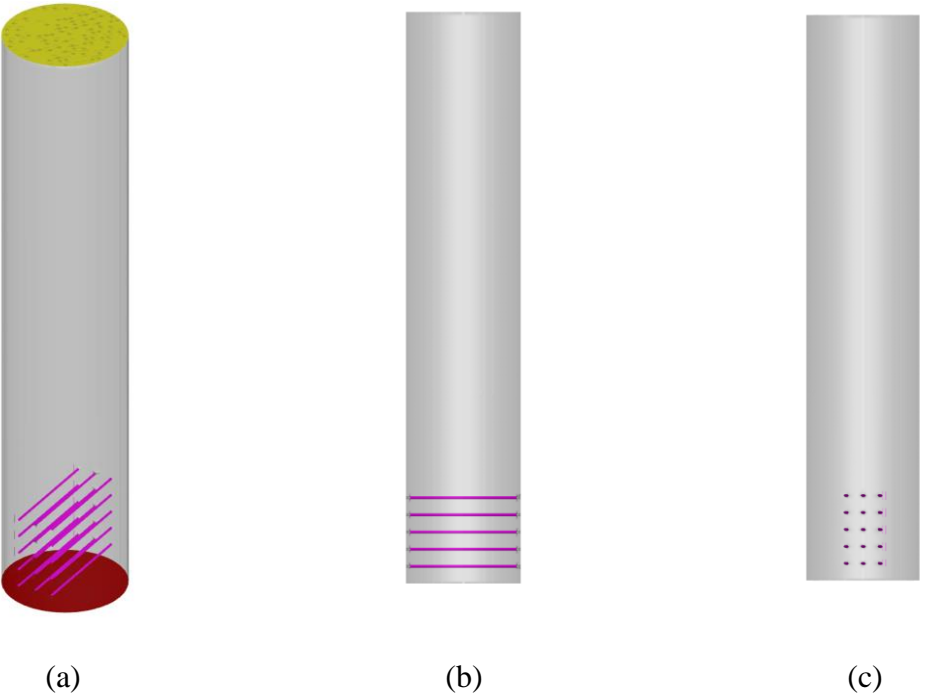


Figure 4.3: Horizontal cooling tubes alignment (a) x-y-z view, (b) x-z plan, (c) x-z plan.

## 4.6 Isothermal simulation for optimizing bed properties.

Fluidization of particles in iso thermal condition is performed where the particle interaction with fluid is observed in various range of parameters value.

### 4.6.1 Simulation setup

Firstly, the CAD model is imported to the CFPD Barracuda VR<sup>®</sup> and the mode need to be fit with CAD file dimension and display dimension. Some excellent feature available in the software interface which can be used to modify the grid lines. The cell numbers indicate the minimum computation unit and for uniform grid set up it is 100000 which finally counts about 94600 to 96500 based of the internal cooling tube design. Figure 4.4 shows the (a) CAD model, (b) flux plane, (c) data points, (d) combined grid and CAD model of the gas cooler.

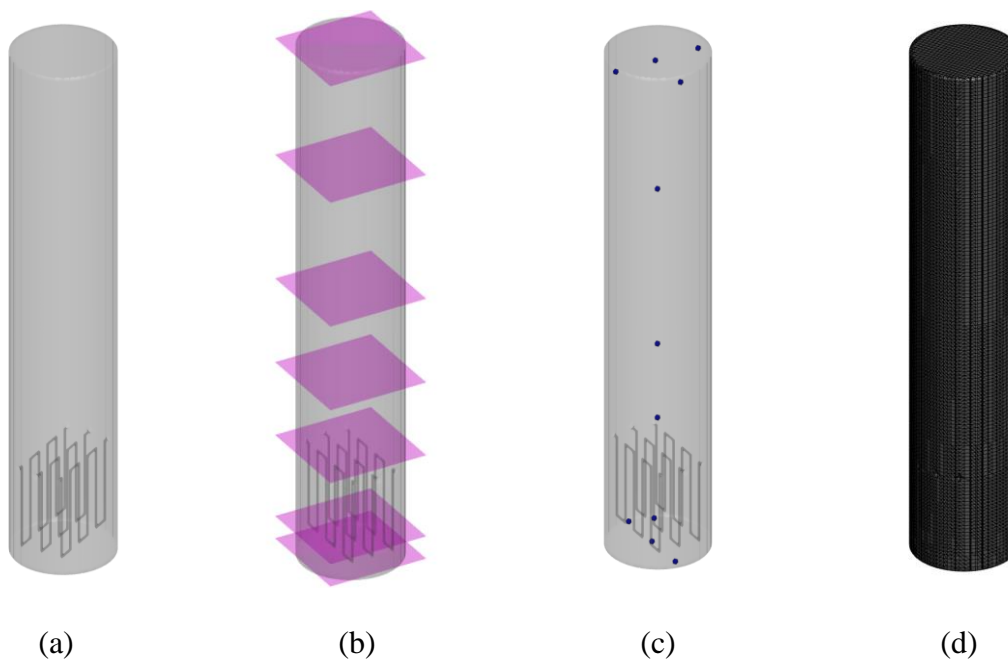


Figure 4.4: (a) CAD model, (b) flux plane, (c) data points, (d) combined grid and CAD model.

**Gridding and grid checking:** Uniform grid is setup for all over the structure. Some modification also done to capture the internal structure in the cylindrical body. This modification provides maximum actual cells for calculation. The final grid also checked, and the figure (b) shows that it is in the acceptable limit.

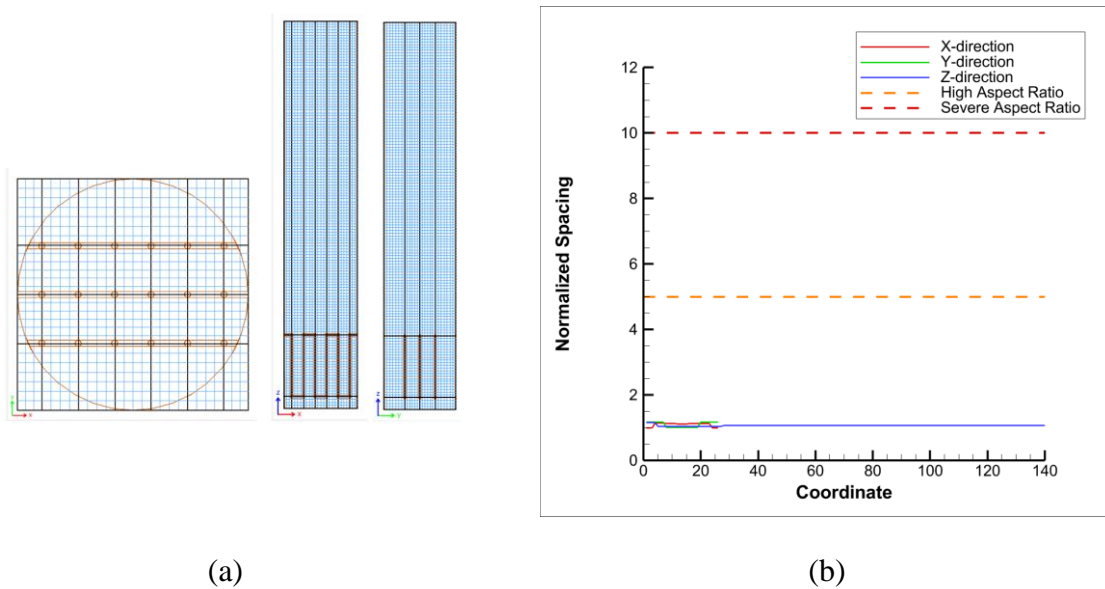


Figure 4.5: Uniform grid setup and grid checking on Barracuda VR<sup>®</sup>.

**Global setting:** This interphase as figure 4.6 is used to select the gravity setting as well as the direction of gravity. Overall thermal setting starts also from here where iso thermal indicate uniform temperature all over the body and non-isothermal is used for thermal effect on process.

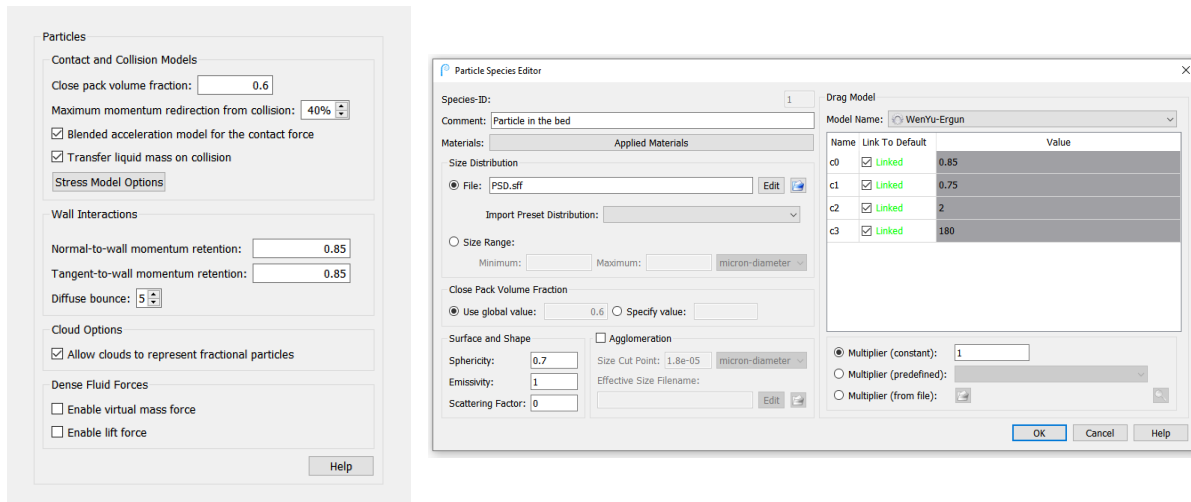
Figure 4.6 shows the Global Settings setup interface. The settings are as follows:

- Global Settings:**
  - Flow Type: Compressible
  - Fluid domain can contain: Gases and vapors
  - Particles can contain: Solids, liquids, and volatiles
  - Bubbles are not available for compressible simulations.*
- Gravity Settings:**
  - x-direction: 0 m/s<sup>2</sup>
  - y-direction: 0 m/s<sup>2</sup>
  - z-direction: -9.81 m/s<sup>2</sup>
- Thermal Settings:**
  - Isothermal
    - Temperature: 673 K
  - Thermal
  - Heat Transfer Coefficients
  - Radiation Model:
    - None
    - Near wall
    - P-1
    - Cap exposed particle area
  - Temperature Warning Limits:
    - Minimum: 100 K
    - Maximum: 6000 K
    - Record minimum and maximum temperatures in MinMaxTemp.data log file
- Simulation Start Options:** (Section header)

Figure 4.6: Global settings setup.

**Base materials setting:** The materials need for the simulation process are available to select in material properties library in this interphase. Material properties can also be edited according to requirement both default and manual input.

**Particles properties:** Particle properties in the bed are defined by the particle properties editor figure 4.7. Drag model and PSD is required to input and other particle properties like sphericity emissivity etc. also needful.



(a)

(b)

Figure 4.7: Particle properties editor (a) & (b).

**Initial condition:** Both particle and fluid initial condition should be input according to the requirement. The cell region can be selected by navigating Fluid IC Editor or Particle IC Editor shows in figure 4.8.

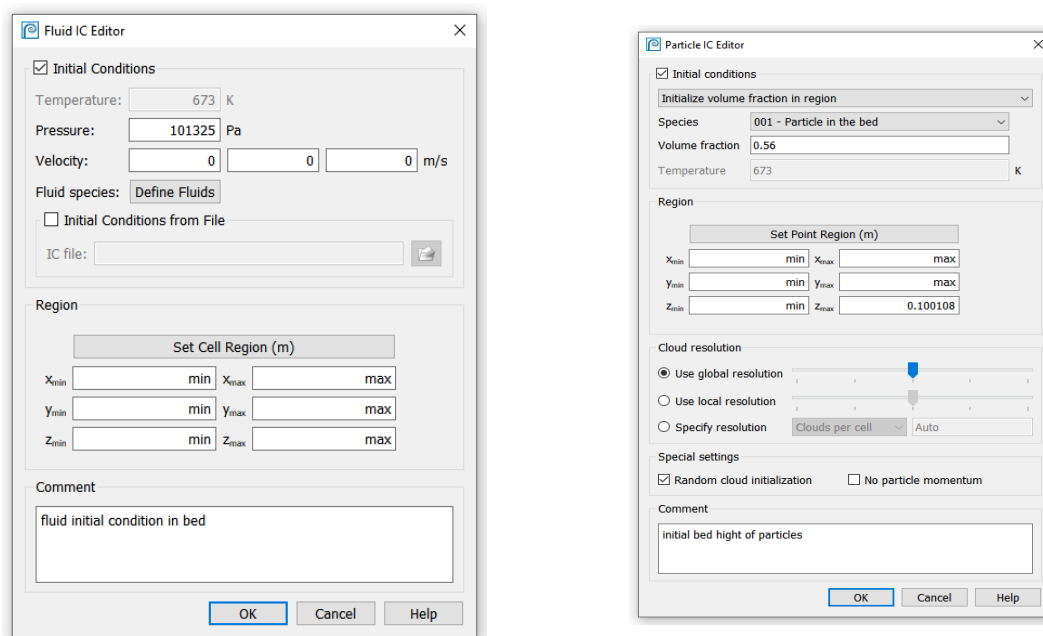


Figure 4.8: Fluid initial conditions and particle initial conditions in bed.

**Boundary condition:** The following figures 4.9 shows the boundary condition where figure 4.10 pressure boundary as well as flow boundary is defined as required for simulation cases. All the direction is selected as Z-direction and particle out flow is allowed for all cases.

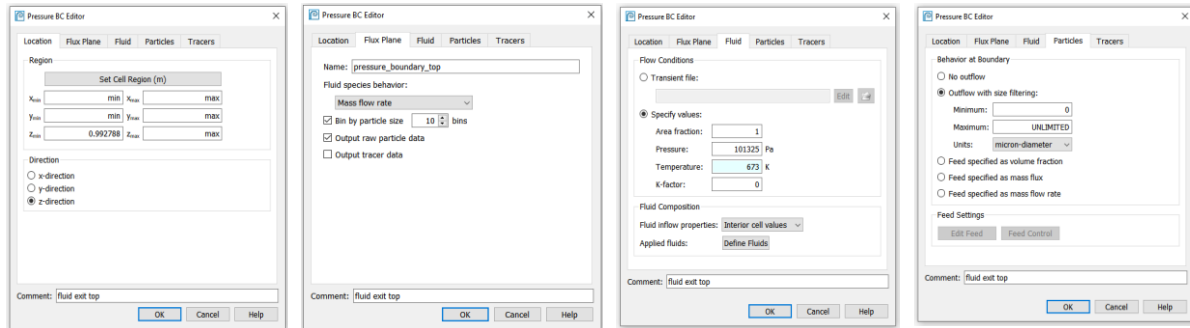


Figure 4.9: Pressure boundary setting.

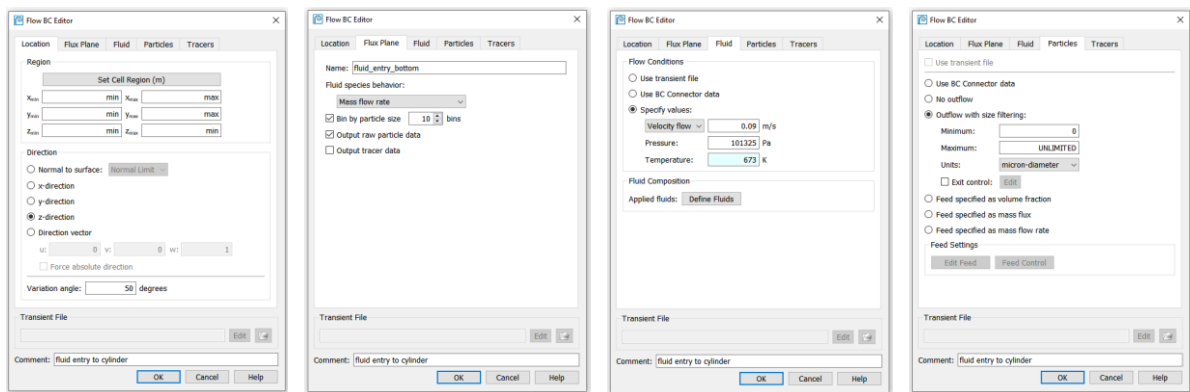


Figure 4.10: Flow boundary setting.

**Simulation time setup:** Both simulation time and the time steps are crucial for simulation. Very little time steps may provide better outputs but takes longer real time. The total simulation time may vary from case to case, but it should be sufficient to obtain optimum result. All the cases of this study are done for time steps 0.005 s. the following figure 4.11 show the interface.

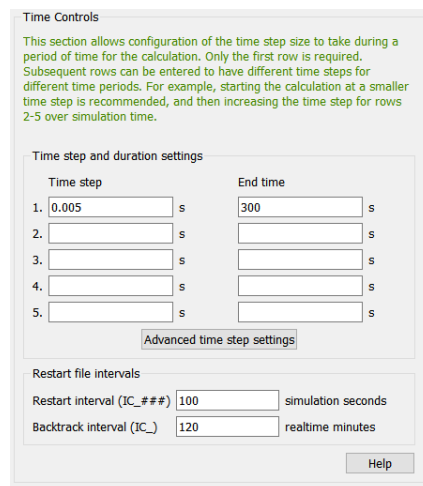


Figure 4.11 Time-control setting.

## 4.6.2 Simulation cases for isothermal

The following table 4.1, 4.2 and 4.3 contains the data of several simulation conditions which are used to simulate for finding geometrical parameters.

Table 4.1: Simulation parameters value for optimizing H/D ratio.

Case no.	Superficial gas velocity ( $m/s$ )	Bottom surface area of cylinder ( $m^2$ )	Diameter of cylinder ( $m$ )	Height of cylinder ( $m$ )	H/D ratio	Volume of bed ( $m^3$ )	Mass of particles in bed ( $kg$ )
Simulation A01	0.9	0.03135	0.1998	0.0999	0.5	0.003132	5.951303
Simulation A02				0.1998	1.0	0.006265	11.90261
Simulation A03				0.2997	1.5	0.009397	17.85391
Simulation A04				0.3996	2.0	0.012529	23.80521
Simulation A05				0.4995	2.5	0.015661	29.75651

Table 4.2: Simulation parameters value for optimizing superficial velocity.

Case no.	Superficial gas velocity ( $m/s$ )	Bottom surface area of cylinder ( $m^2$ )	Diameter of cylinder ( $m$ )	Hight of cylinder ( $m$ )	Volume of bed ( $m^3$ )	Mass of particles in bed ( $kg$ )
Simulation B01	0.05	0.031354	0.1998	0.3997	0.01253	23.8052
Simulation B02	0.07					
Simulation B03	0.09					
Simulation B04	0.11					
Simulation B05	0.13					

Table 4.3: Simulation parameters value for optimizing bottom surface area of cylinder.

Case no.	Superficial gas velocity ( $m/s$ )	Bottom surface area of cylinder ( $m^2$ )	Diameter of cylinder ( $m$ )	Height of Bed ( $m$ )	Volume of bed ( $m^3$ )	Mass of particles in bed ( $kg$ )
	$m/s$	$m^2$	$m$	$m$	$m^3$	$kg$
Simulation C01	0.9	0.056438	0.268065	0.3997	0.022558	42.86071
Simulation C02		0.040313	0.226557		0.016113	30.6149
Simulation C03		0.031354	0.199803		0.012532	23.81117
Simulation C04		0.025654	0.180731		0.010254	19.48242

## 4.7 Thermal Simulation for optimizing cooling capacity.

The thermal effect of the fluidized bed is optimized in the CPFV Barracuda VR<sup>®</sup>. The previously obtained geometry is used to study further with active internal cooling tubes. Simulation is performed for 500 seconds, and post processing of the data is used to observe the outputs.

### 4.7.1 Simulation setup

Non-isothermal simulation provides the thermal study based on input data. Previous section 4.6 is similar to many of the interphase setting and rest is tuned as follows.

**Global setting:** This option allows to input the data related to the temperature change in the process. Fluid to wall heat transfer and fluid to particle heat transfer co-efficient is calculated by default according to the equation discuss in section 3.5. there also three available options for radiation model but for this study it is assumed as zero.

Figure 4.12: Global setting for non-isothermal condition.

**Thermal wall boundary condition:** Gas cooler contains cooling tubes inside the cylindrical structure. Three cooling tubes are designed and arranged both horizontal and vertical alinement. Thermal wall BC editor provides various option to input data like wall temperature of tube, surface area of tubes and region of tubes by selecting the cell area in Barracuda VR<sup>®</sup> window. The direction is selected as normal to the surface and emissivity value as unity as default. The following figure 4.13 shows the three cooling tubes thermal setting in software.

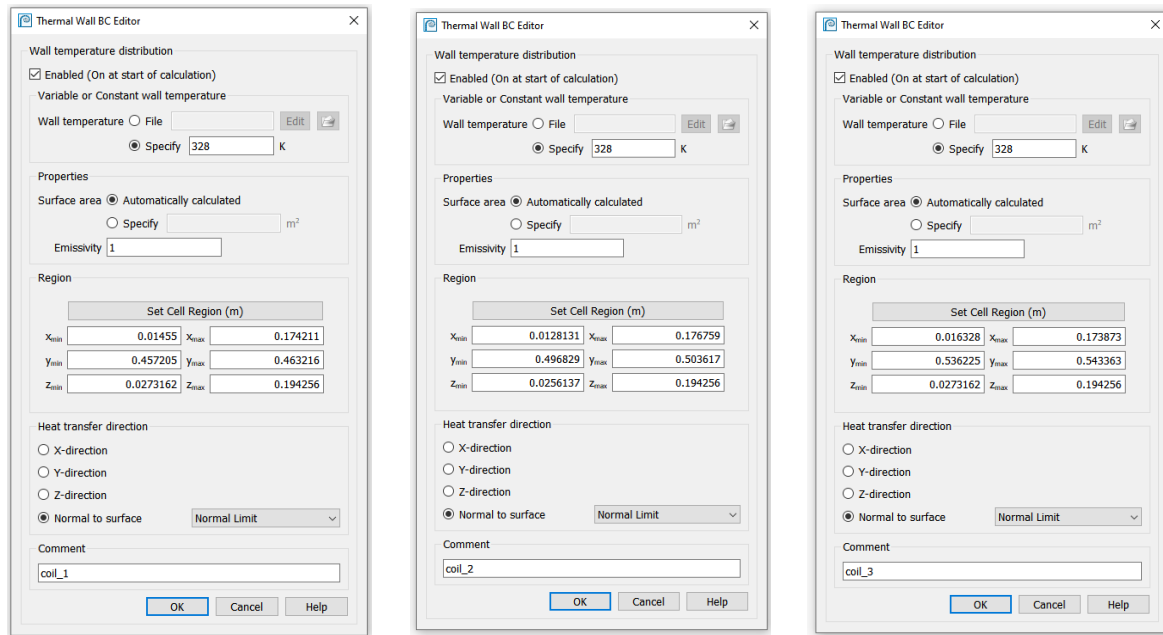


Figure 4.13: Thermal cooling tube setting.

#### 4.7.2 Simulation cases for non-isothermal

Several cases are performed as described follows where both horizontal and vertical alignment of tubes are considered. The following table 4.4 and 4.5 show the conditions of simulations.

Table 4.4: Simulation cases for horizontal cooling tube in the bed.

Case no.	Temperature of coolant		Remarks
	inlet (K)	outlet (K)	
Simulation V01	30	80	H/D=1.0
Simulation V02	30	80	Bed materials at 293 k IC.
Simulation V03	30	80	H/D=2.0

Table 4.5: simulation cases for horizontal cooling tube in the bed.

Case no.	Temperature of coolant		Remarks
	inlet (K)	outlet (K)	
Simulation H01	30	80	H/D=2.0



## 5 Result and discussion

This chapter describes the obtained result of different simulations conducted in CPFDD Barracuda VR<sup>®</sup>. The output is discussed according to the simulation conditions. Firstly, the isothermal simulation is performed to optimize the fluidized bed parameters. These parameters provide ideas to construct the geometry of the gas cooler. Finally, the non-isothermal simulation reveals the thermal interaction among the particles, fluid, and walls of gas cooler.

### 5.1 Particles size distribution

Particles are the core things on which the overall fluidization performance depends. This study considers the alumina as the bed particles as recommended in the thesis. Appendix D shows the particles properties provided by an external partner collaborating on the thesis, Hydro Aluminum AS. The range of particles in the collection is referred to as particle size distribution. The data used for this study is obtained from them. The following figure 5.1 shows the particle size distribution calculated based on the given data and according to the calculation refers to the appendix A.

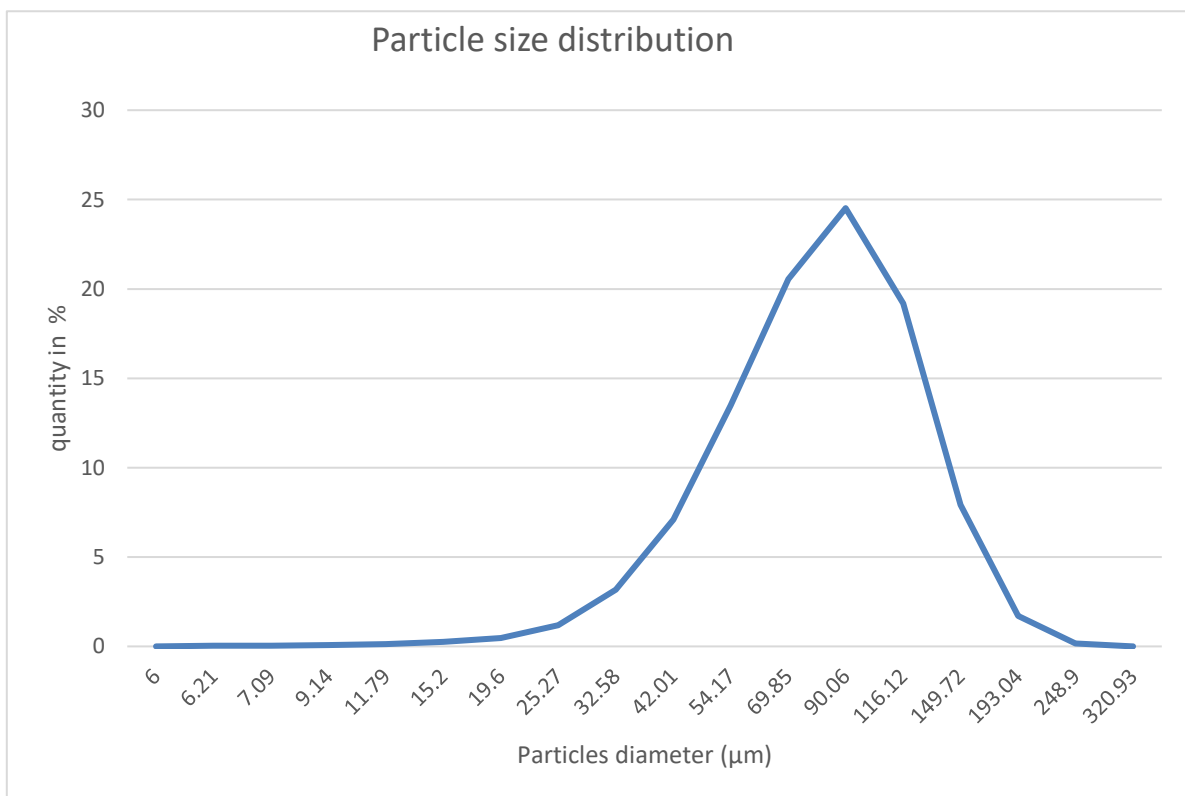


Figure 5.1: Particle size distribution.

## 5.2 Fluidized gas properties

Fluidization gas properties are also important parameters depending on the nature of gas. Carbon di oxide (CO<sub>2</sub>) is considered as a fluidization gas. The gas properties like density, viscosity etc. are considered at 400 °C which was automatically calculated by the software. The following table shows the gas properties used in this work.

Table 5.1: Carbon-di-oxide properties calculated according to appendix B.

Parameters	Unit	Value
Density ( $\rho_g$ )	$kg/m^3$	0.7874923
Viscosity ( $\mu_g$ )	$N.s/m^2$	2.95871E-05
Heat capacity ( $C_{p,g}$ )	$j/kg.K$	1.11389

## 5.3 Fluidized gas velocity

The following table contains the calculated data according to the equations discussed earlier. The superficial velocity of different is calculated based on the given data and other gas and particles properties in considered temperature.

Table 5.2: Fluidized bed properties.

Parameters	Used equation number	Obtained value	unit
Minimum fluidization velocity	(3.8)	0.00156	$m/s$
Minimum bubbling velocity	(3.9)	0.03239	$m/s$
Terminal velocity of particles	(3.10)	0.14927	$m/s$

### 5.3.1 Bed diameter, height, bottom surface area, bed static volume and amount of bed material calculation

A cylindrical structure is considered as a basis for further calculation and design, other possible structure is not studied. Therefore, the fluidized bed diameter, bed height, the bottom surface area of cylinder as well as the static volume of bed material is calculated for every possible case to simulate in Barracuda VR. All the calculations of these properties are based upon the range of superficial velocity ( $u_{sf}$ ) from minimum bubbling velocity ( $u_{mb}$ ) to terminal velocity ( $u_t$ ) to find out optimum bubbling fluidized bed of taken particles size distribution.

The fluidized bed diameter is simply calculated according to following equation.

$$D_{FBR} = \left( \frac{4\dot{v}_f}{u_{sf} \cdot \pi} \right)^{\frac{1}{2}} \quad (5.1)$$

Where  $D_{FB}$  is fluidized bed diameter,  $\dot{v}_f$  is the volumetric flowrate of gas.

Bottom surface area ( $A_{cylinder's\ bottom}$ ) of the cylinder is calculated by the equation bellow and several cases are simulated in purpose of finding optimum geometry.

$$A_{cylinder's\ bottom} = \frac{r}{4} \cdot D_{FB}^2 \quad (5.2)$$

Bed static volume and total bed material or the amount of alumina used in the bed for several cases are determined according to following.

$$V_{FB} = A_{cylinder's\ bottom} \cdot H_{BED} \quad (5.3)$$

Here  $V_{FB}$  is the volume of the static bed,  $H_{BED}$  is the static bed height.

The total mass of the alumina in the bed is the calculated by multiplying the volume of bed to particle envelop density which is taken as  $1900\text{ kg/m}^3$ .

$$M_{FB} = 1900\text{ kg/m}^3 \cdot V_{FB} \quad (5.4)$$

Where,  $M_{FB}$  is the mass of the particles in the bed.

## 5.4 Cooling performance calculation

According to the given data the total available heat of the gas cooler and other parameters are calculated by using the equations discussed in chapter (4.2) and appendix B. The overall heat transfer co-efficient is assumed as  $100\text{ W/m}^2\cdot\text{K}$ . The following table shows the calculated values of different parameters.

Table 5.3: Thermal calculation of various parameters.

Parameters	Used equation number	Unit	Value
------------	----------------------	------	-------

Cooling load ( $Q_{total}$ )	(4.3)	$J/s$	742.6
Heat transfer surface area ( $A_{tube}$ )	(4.11)	$mm^2$	49500
Cooling tubes length ( $l$ )	(4.12)	$mm$	3152
Coolant flowrate ( $\dot{m}_{water}$ )	(4.4)	$kg/h$	12.78

## 5.5 H/D ratio of the bed

Height to bed ratio in range of 0.5 to 2.5 is considered to performed in simulations. The overall particles outflow is observed at the top of the cylindrical body. The simulation time was 300s and particles in the bed are observed. The following figure shows various H/D ratio and particles distribution in the bed.

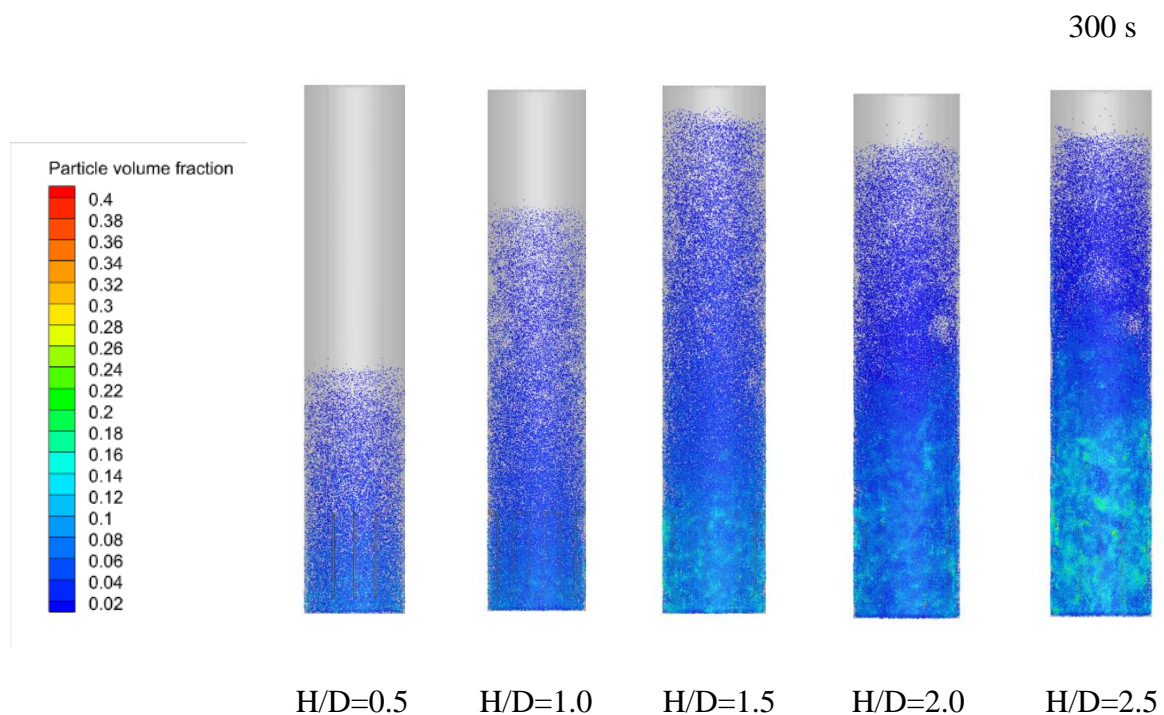
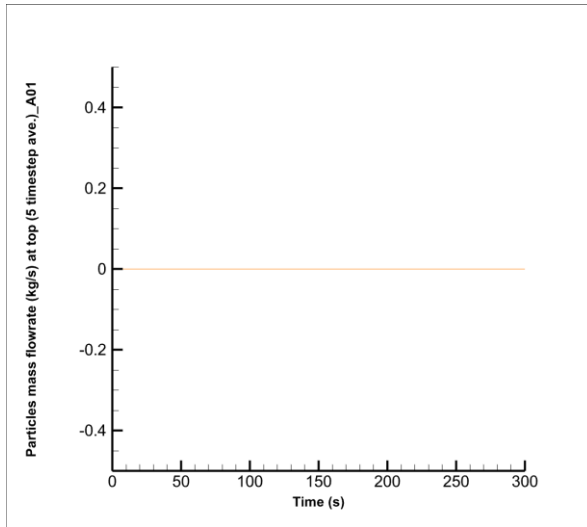


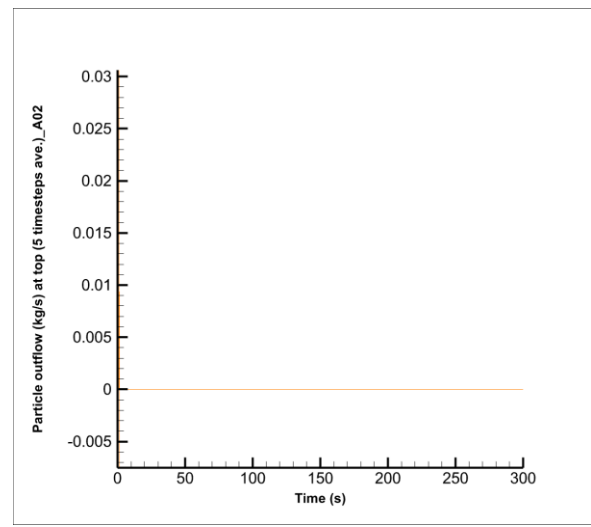
Figure 5.2: Particles distributions throughout the bed.

The following graph figure 5.3 shows the five simulations conducted in the software where the inlet gas flowrate and bottom surface area of the cylinder are maintained constant as 0.09 m/s and 0,031354 m<sup>2</sup> respectively. Simulation\_A01 and simulation \_A02 shows the zero outflow of the particle at the top. The simulation \_A03, A04 and A05 reveal particles outflow at top of cylinder.

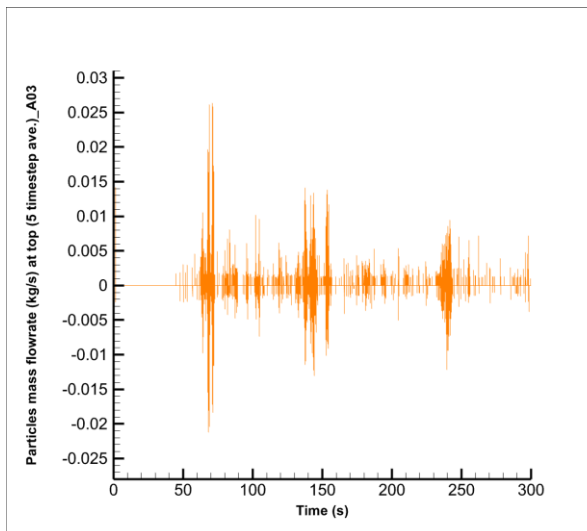
## 5 Result and discussion



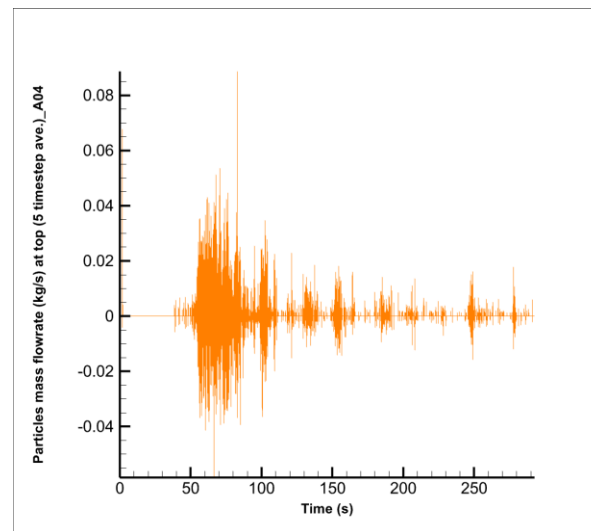
(a) Simulation A01



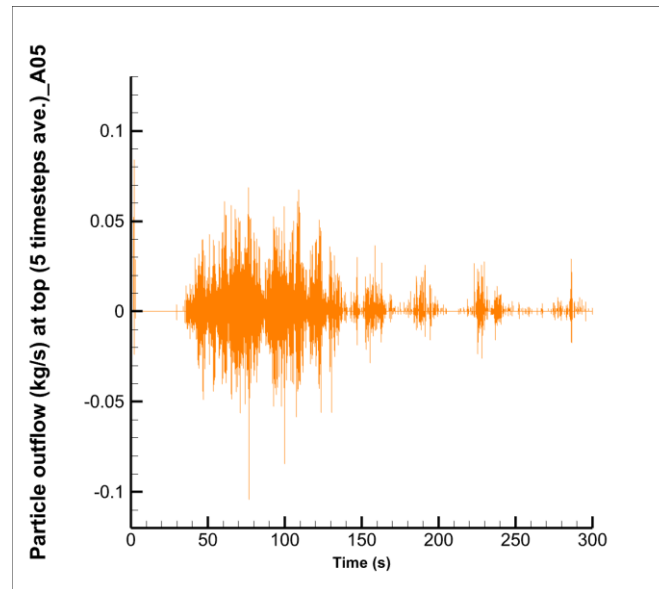
(b) Simulation A02



(c) Simulation A03



(d) Simulation A04



(e) Simulation A05

Figure 5.3: Particle out flow for simulation\_A01, A02, A03, A04 and A05.

The below figure 5.4 shows the time integrated mass of all species with time. According to the plot, Simulation\_A05 gives the largest amount of particles outflow of the cylinder which is about 0.18 kg. Simulation\_A04 and A03 have outflow about 0.09 kg and 0.02 kg respectively. Rest two simulation have zero outflow of particles.

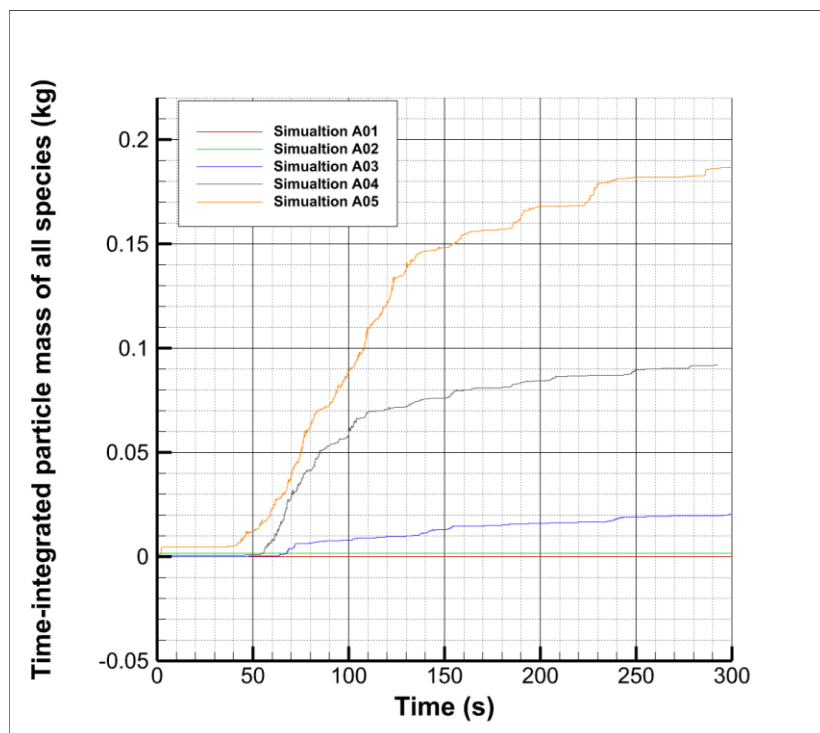


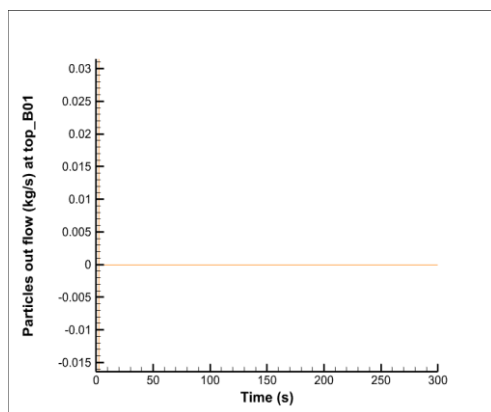
Figure 5.4: Time-integrated particle mass of all species.

## 5 Result and discussion

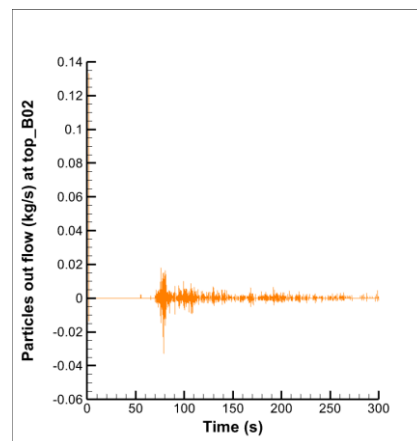
Here the graph supports taking the H/D ratio in a range of 1.0 to 2.0. less than the H/D ratio 1.0 the above figure 5.4 shows there are less bed expansion and total bed height become too small to insert the cooling tube (see figure 5.2). The less height also says the less particles in the bed fluidize and less interaction for heat transfer. On the other hand, a larger H/D ratio than 2.0 shows a large amount of particle go out of the cylinder. This range is taken later for thermal simulation of the fluidized bed.

### 5.6 Optimum superficial velocity

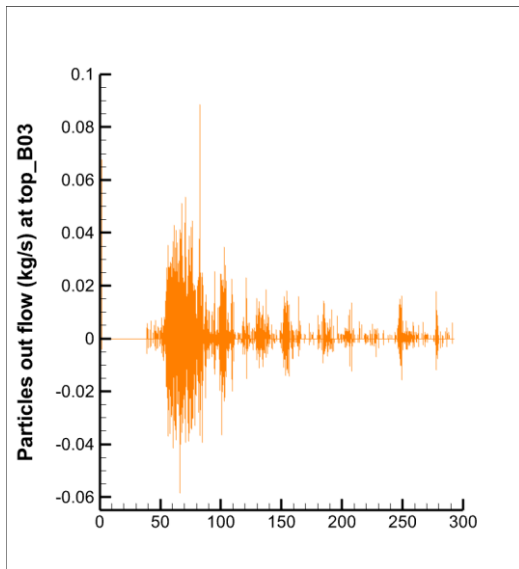
The superficial velocities used in the fluidization of the particles are considered in between the minimum bubbling velocity to the terminal velocity. Within the range five simulation are conducted to observe the particle s distribution in the fluidized bed as well as the particle out flow at the top. The following five graph of figure 5.5 shows the particle outflow at top of the cylindrical body of gas cooler. Simulation\_B01 represent the superficial velocity of 0.05 m/s and the simulation\_B02, B03, B04 and B05 represent superficial velocity of 0.07 m/s<sup>2</sup>, 0.09 m/s<sup>2</sup>, 0.11 m/s<sup>2</sup>, 0.13 m/s<sup>2</sup> respectively. All the simulations run for 300 seconds.



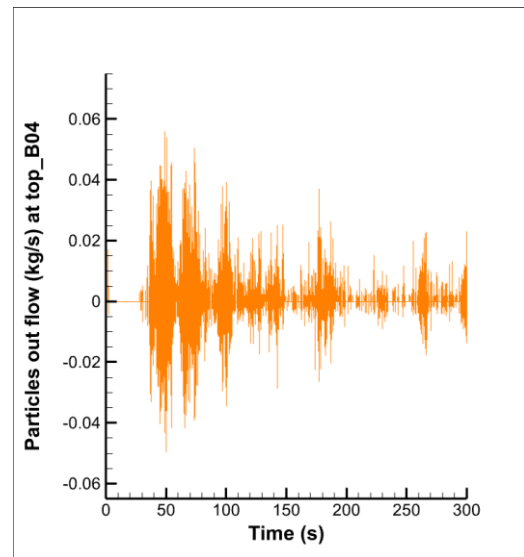
(a) Simulation B01



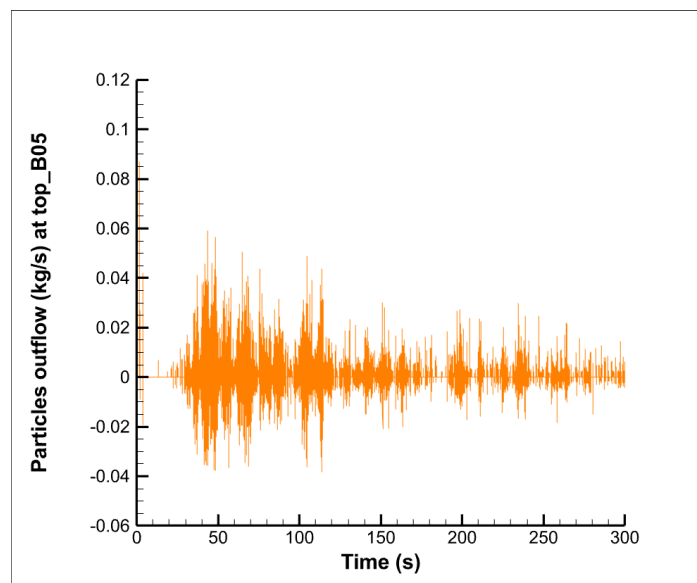
(b) Simulation B02



(c) Simulation B03



(d) Simulation B04



(e) Simulation B05

Figure 5.5: Particle out flow for simulation\_B01, B02, B03, B04 and B05

Cumulative particle mass outflow is shown in figure 5.6 below. Simulation\_B01 represent the lowest superficial velocity and simulation\_B05 is for highest superficial velocity close to terminal velocity. The simulation\_B05 indicate the highest amount of particle 0.16 kg go out from the cylinder, after that simulation\_B04, in which the amount is 0.14 kg. Zero particle out flow is shown by simulation\_B01 for superficial velocity of 0.05 m/s but this also create less turbulence in the bed. Considering the better hydrodynamics and minimum particle outflow simulation\_03 can be considered as the optimum for the process which is 0.09 m/s.



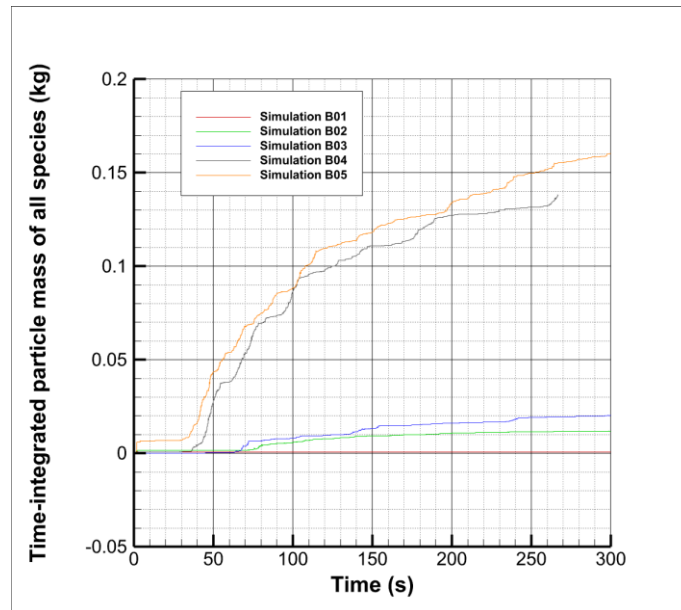
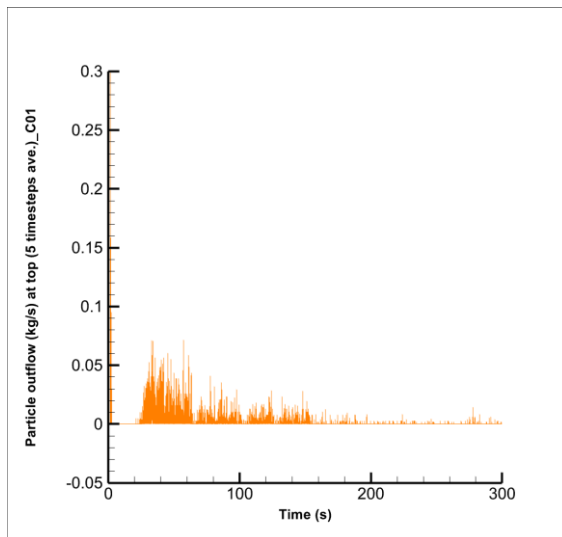


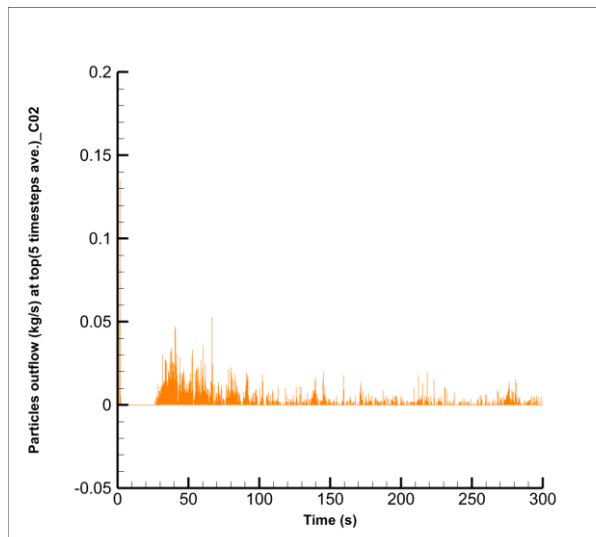
Figure 5.6: Cumulative particle mass out flow for 300 s.

## 5.7 Optimum area

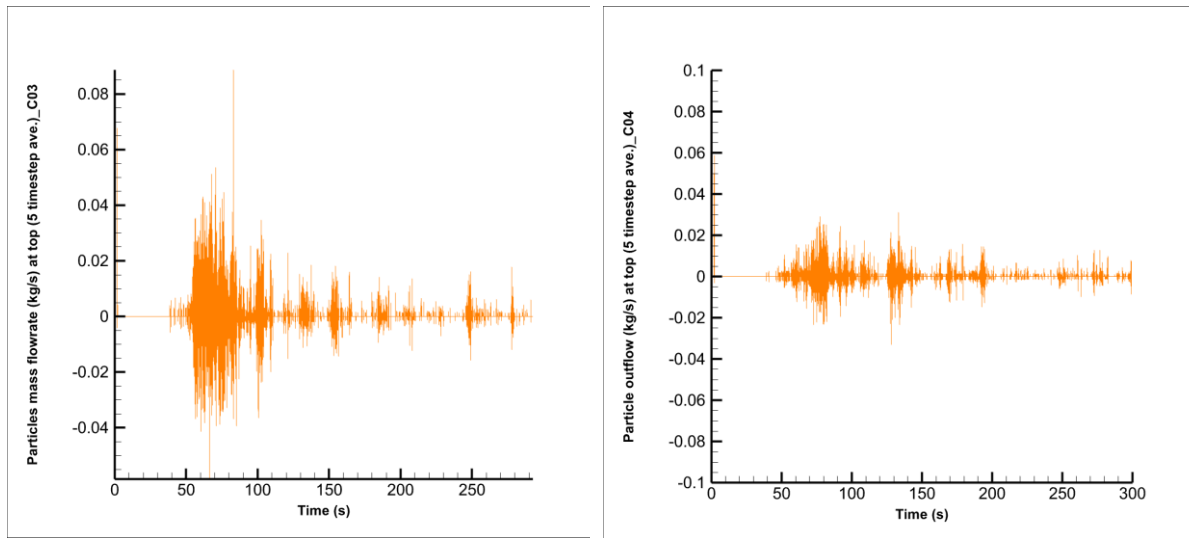
The bottom surface area of the cylindrical body is also simulated by keeping the bed height constant which provide the mass of the bed materials for the fluidization bed. Four simulations are performed to observe the particle distributions and expansion of static bed.



(a) Simulation C01



(b) Simulation C02



(a) Simulation C03

(a) Simulation C04

Figure 5.7: Particle out flow for simulation\_C01, C02, C03, and C04.

The above figure 5.7 shows the simulation result which indicate bottom surface area of cylindrical bed of  $0.056438 \text{ m}^2$ ,  $0.040313 \text{ m}^2$ ,  $0.031354 \text{ m}^2$  and  $0.025654 \text{ m}^2$  respectively. This finding says that every simulation provides very less out flow of particles.

## 5.8 Heat transfer performance

Several simulations are conducted to find thermal performance of the gas cooler. Both vertical and horizontal alignment of internal cooling tubes system is performed in Barracuda VR<sup>®</sup> 23.1.0 version and obtained data is processed for graphical representation.

### 5.8.1 Vertical cooling tubes performance

**Simulation\_V01:** This case of the simulation used the coolant available at  $30 \text{ }^\circ\text{C}$  and outlet coolant temperature assumed as  $80 \text{ }^\circ\text{C}$ . The following figure 5.8 shows the overall heat transfer rate as well as the heat transfer rate of individual cooling tubes inserted into the dense phase of the fluidized bed. The overall cooling load obtained from the graph is about  $750 \text{ J/s}$  where individual three cooling tubes shows about  $220 \text{ J/s}$  each. The graph also reveals that the gas cooler of this conditions takes about  $280 \text{ s}$  to reach the equilibrium performance at which the operation of the gas cooler should be stable. The negative sign of the plot value refers to the fluidized system releases thermal energy to the coolant.

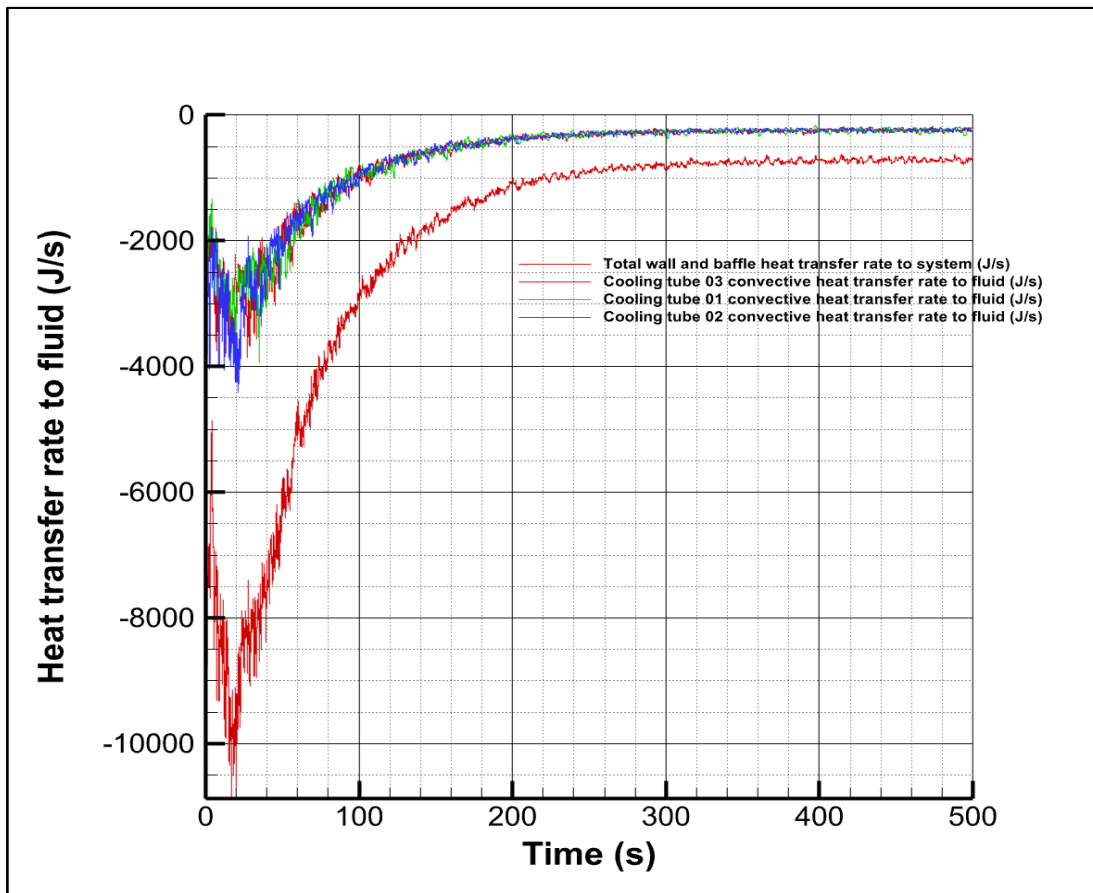


Figure 5.8: Heat transfer rate for vertical tubes.

Below figure 5.9 shows the average fluid temperature at the top of the cylinder over time. Here this is clearly seen that the fluid temperature goes down during simulation of this case. The initial temperature of the fluid was 673 K which takes about 280 seconds to reach a constant outlet fluid temperature close to 360 K and continuation of the graph confirms the operating stability of the system.

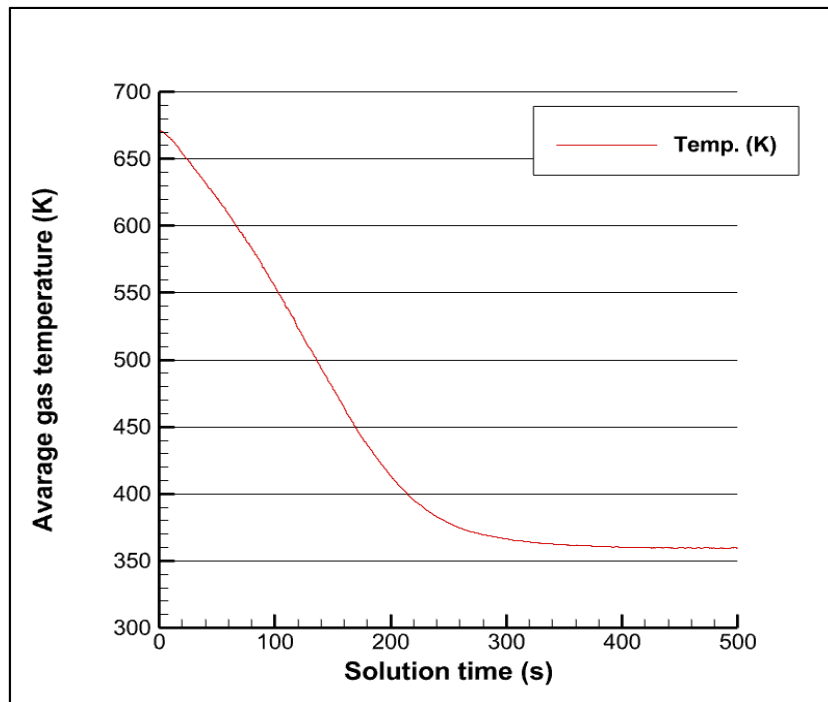


Figure 5.9: Average temperature at top of the gas cooler.

Time integrated heat transfer for simulation\_V01 at figure 5.10 shows the value of total heat transfer is approximately 10,00,000 J for 500 seconds. The graph is rapidly high at the beginning of simulation and later changes gradually as the heat transfer rate tends to be stable.

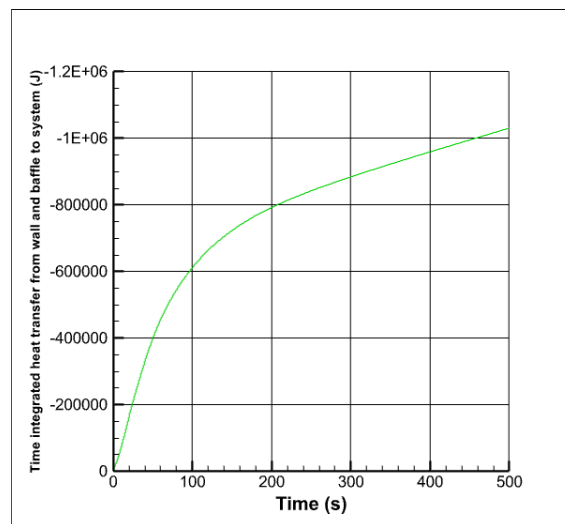


Figure 5.10: Time integrated heat transfer of cooling tubes.

Pressure of the fluid at top of the cylinder also change due to inlet gas interaction with the particles in the bed. Figure 5.11 shows the pressure curve for time zero to 500 seconds where the gas pressure drops rapidly in the beginning and maintain stable curve after 200 seconds.

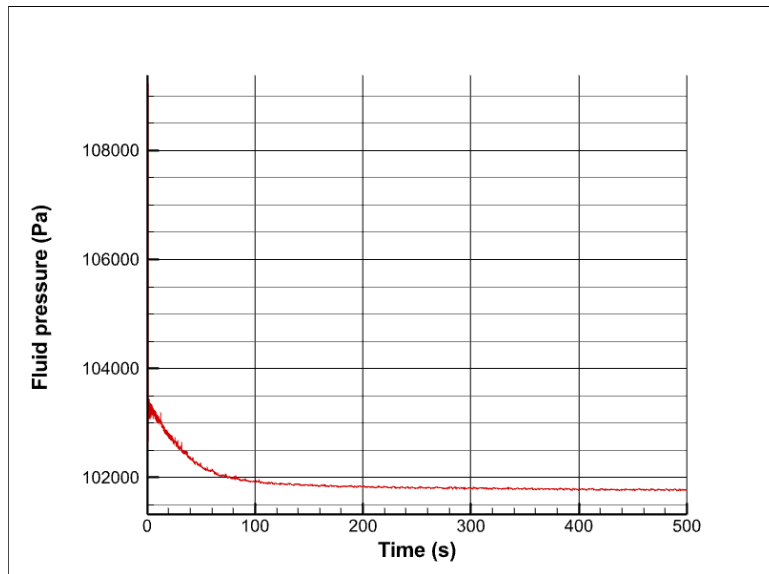


Figure 5.11: Gas pressure at top of cylinder.

The following figure 5.12 shows the temperature profile over time. The initial temperature change over time and reach to about 360 k in stable conditions.

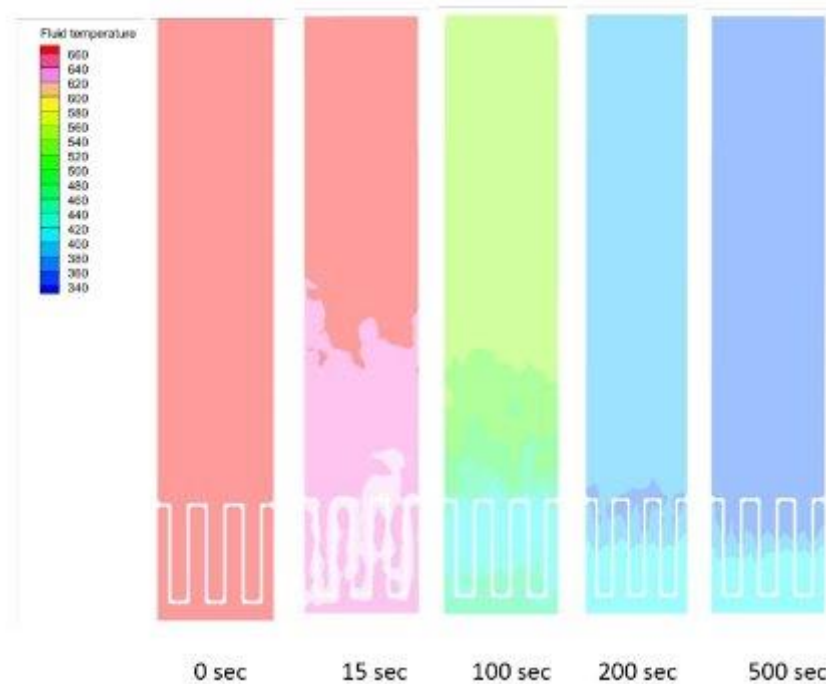


Figure 5.12 : fluid temperature profile over time.

The following figure 5.13: shows the particles temperature changes over time. The initial temperature of the particles was 673 k and after 230 sec its reach to temperature about 360 k.

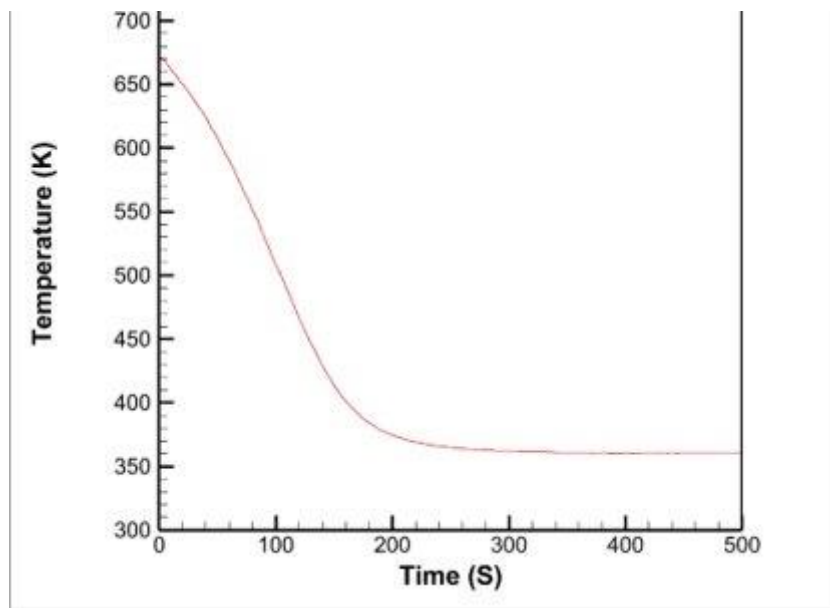
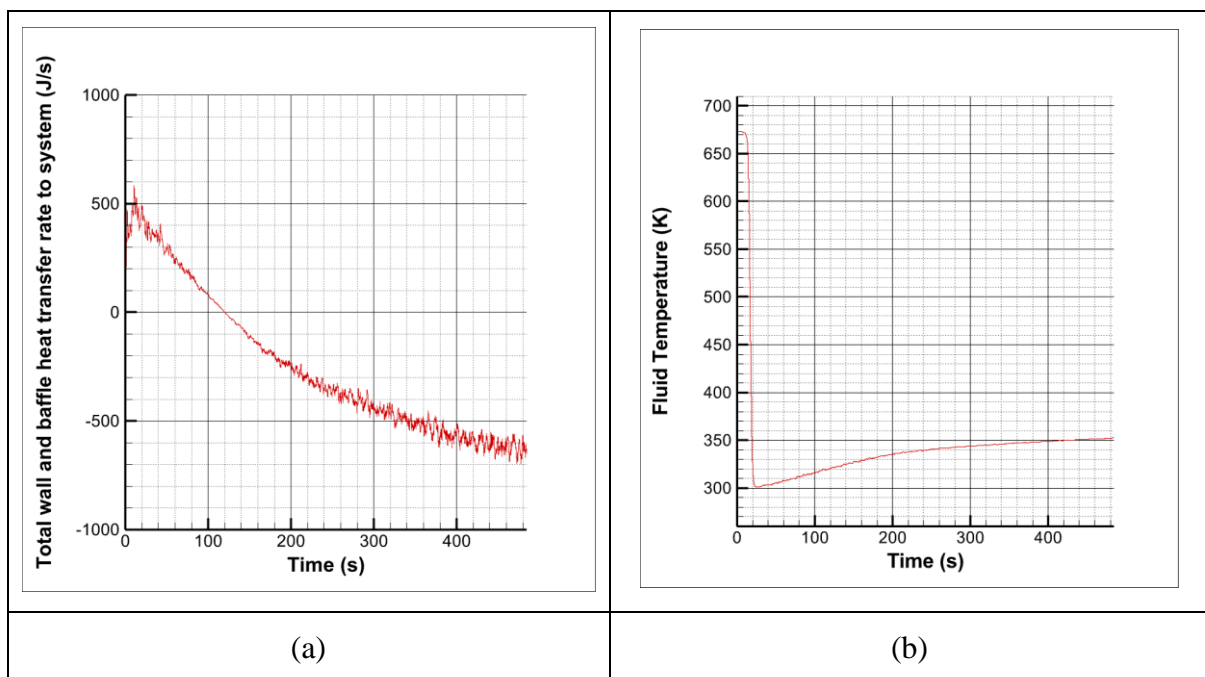


Figure 5.13: Particle temperature changed over time.

**Simulation\_V02:** The simulation of this case use the H/D ratio 1.0 and the initial particle temperature is 293 K. The following graph in figure 5.14 shows (a) the total heat transfer rate of the system, (b) gas temperature at the top of cylinder, (c) time integrated heat transfer from wall to system and (d) the pressure from initial to final simulation time.



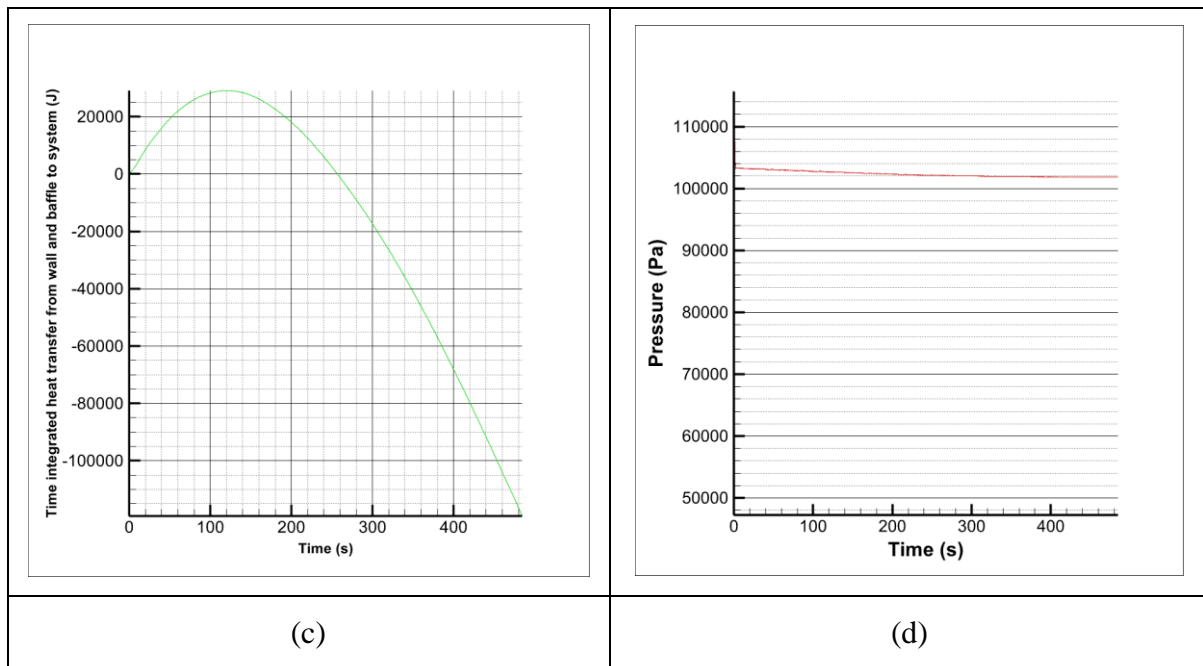


Figure 5.14: Simulation outputs (a) heat transfer rate of system, (b) Gas temperature at outlet, (c) time integrated heat transfer (d) pressure of gas.

As the particle temperature (293) input is lower than the gas inlet temperature (673 K), the graph shows that the thermal energy transfer from gas to particle in the bed is positive. Later these turns to negative direction which indicate the thermal energy flow out of the system by coolant (average temperature 328 K). the time integrated heat transfer also takes about 250 s to turn toward negative direction figure 5.14 (c). pressure changes very little during the simulation figure 5.14 (d) whereas the fluid temperature changes significantly from 673 K to 350 K and this takes about 380 seconds to be stable. Figure 5.14 (d) shows instant change of gas inlet temperature due to gas to particles heat transfer happening rapidly in the fluidized bed. time integrated heat transfer shows that total heat transfer after 500 seconds is about 12,00,000 J.

**Simulation\_V03:** This simulation for vertical internal cooling tube arrangement is performed with H/D ratio 2.0 that means the total bed materials used here about 23 kg. The simulation run for 500 seconds, and the output of simulation shown at figure 5.15. Figure 5.15 (a) shows the heat transfer rate of the system although the system is not seemed like stable but the trends of the graph takes heat transfer rate at 500 s is about 950 J/s. Fluid temperature obtained at the top of cylinder is about 460 K figure 5.15 (b). the amount of total heat transfer of the system is about 10,00,000 J in 500 s by the graph 5.15 (c).

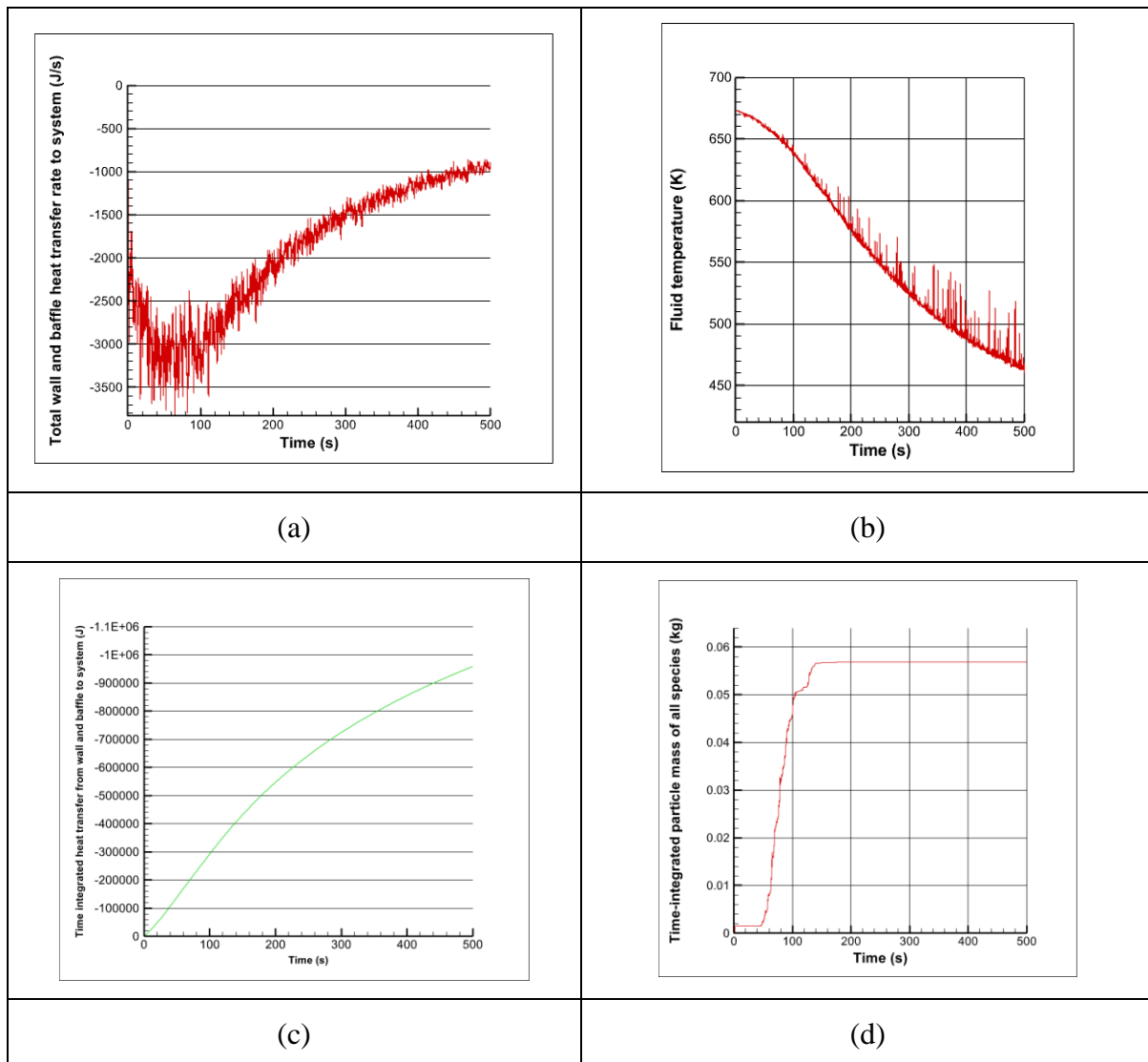


Figure 5.15: Simulation\_V3 (a) heat transfer rate, (b) fluid temperature, (c) Time integrated heat transfer, (d) time integrated mass out flow at top.

### 5.8.2 Horizontal cooling tubes performance

**Simulation\_H01:** Horizontal tubes inserted in the dense phase of the fluidized bed are simulated in this case. The simulation result shown in figure 5.16 where (a) heat transfer rate, (b) fluid temperature at top, (c) time integrated heat transfer. After 250 seconds the heat transfer rate curve nearly stable with in a little range of fluctuations figure 5.16 (a) but the fluid temperature curve still downward in the same trends in figure 5.16 (b) which may go further by increasing simulation time. Time integrated heat transfer shows the value approximately 5,00,000 J in 250 seconds.



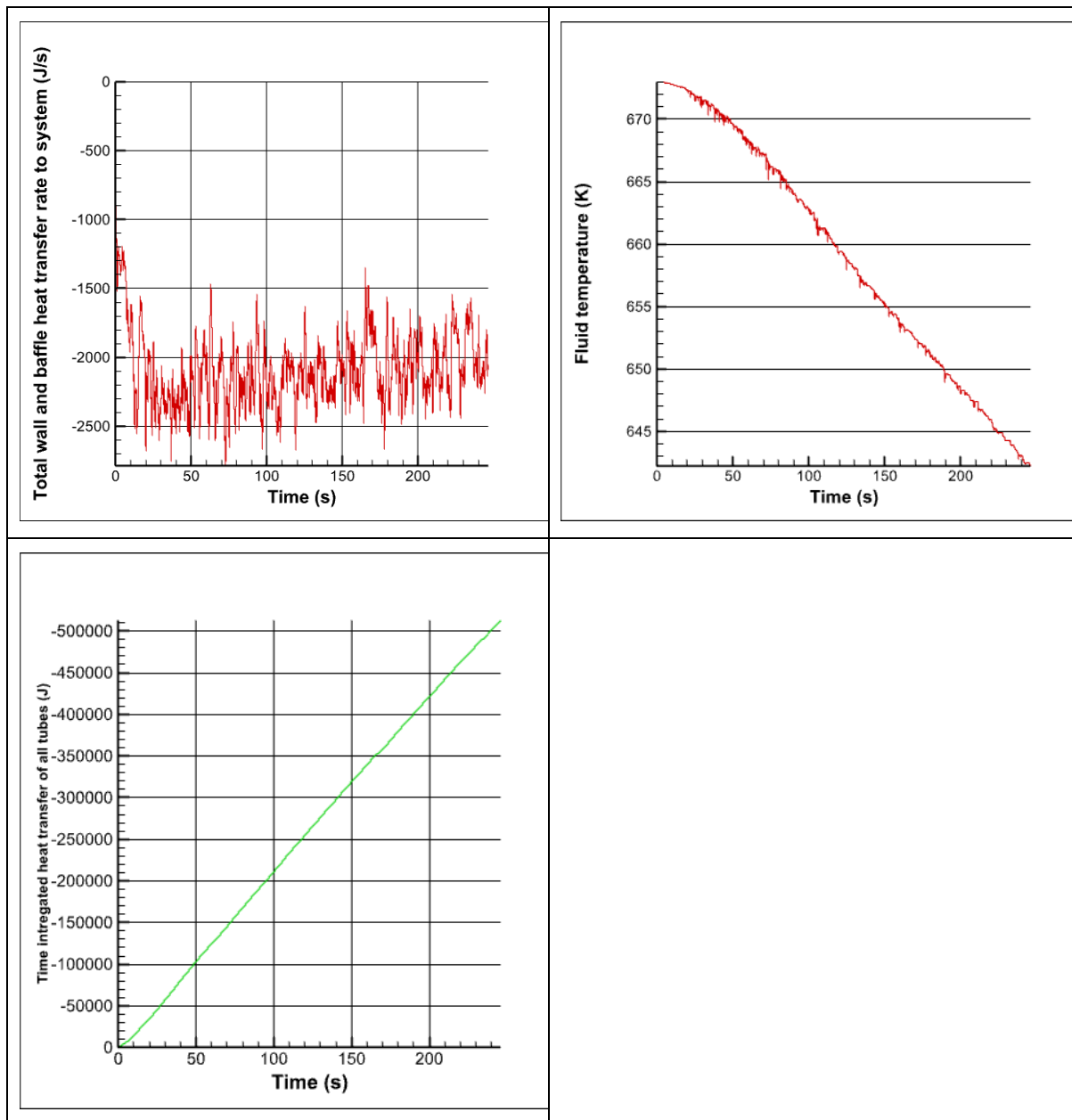


Figure 5.16 Simulation output of horizontal tubes (a) heat transfer rate, (b) fluid temperature at top, (c) time integrated heat transfer.

**Summary of findings:** Various parameters calculated in this study to find the best geometry as well as better heat transfer performance of the gas cooler are reported earlier of this chapter.

The calculation for the heat transfer of the gas cooler unit using the NTU method which give very close result the simulation\_V01 but for more realistic model of fluidized bed heat transfer complex calculation should perform including heat transfer coefficient calculation and other parameters.

The fluidization gas velocity was selected with range of superficial velocity and found the optimum as 0.9 m/s but other velocity close to it also workable. H/D ratio range from 1.0 to 2.0 indicate the particle mass in the bed about 11.9 kg to 23.8 kg respectively. Within this range

## 5 Result and discussion

vertical tubes simulation\_V01 and Simulation\_V03 both performed better than the horizontal simulation\_H01.

Simulation\_H01 show the runtime 250 s which supposed to run 500 s but stop due to unavailable computer storage. So, the result of this simulation is compared with other depending on the run time and plot trends.

In CPFDD Barracuda VR<sup>®</sup> the thermal input setting is considered the average tube surface temperature in between inlet coolant temperature to outlet temperature which is also an approximation this also can be reduced by inserting the temperature range splitting into several segments. The software automatically calculated the heat transfer surface area as well as the heat transfer coefficient based on the model selected for drag force. Grid generation shows the overall geometry may not considered if the part of geometry become very small in the cell in grid generation.

The work presented in the thesis report recommend extending in future to get more realistic model of gas cooler and accurate parameters that's fits practically.

- Cyclone separator and particle collector should attach with presented design to prevent loss of bed materials.
- Fluidized bed simulation data needs to be validated with experiment practically for real system.
- Study with wide range of temperature different of coolant inlet and outlet.
- Different types of calculation and methods like log mean temperature difference (LMTD) requires finding deviation.
- Should study the segment wise temperature input of cooling tube to get more realistic simulation where present study used the uniform temperature all over the tube surface.
- Several tubes arrangement with wide range of temperature should study more for better result.
- Calculation of heat transfer co-efficient (h) for such a system is highly recommended instead of assumption. This will provide more information about design.
- Several structures of fluidized bed column may consider as particles will have more or less space inside the bed.
- The different types of distributor plates should study.

## 6 Conclusion

A fluidized bed gas cooler is an efficient system for thermal control of a process stream. The review of this topic shows that this fluidized bed heat exchanger has multi-applications in various field. The task was to design fluidized bed-based gas cooler as well as the performance calculation with CPFDD Barracuda VR<sup>®</sup>. The geometrical parameters have studied based on given data and later it was simulated on the software. The cooling load, heat transfer area, the internal cooling tubes length and coolant flow rate is found to be approximately 742.6 J/s, 49500 mm<sup>2</sup>, 3221 mm and 12.78 kg/h respectively. Several simulations run in the CPFDD Barracuda VR<sup>®</sup>, and the heat transfer rate also found about 750.0 J/s where the inlet hot gas cools down from 400 °C to about 90-100 °C for H/D ratio 1.0 and a bit more for H/D ratio 2.0 in vertical internal cooling tubes arrangement. Some simulations were also performed to tune the geometrical shape of the gas cooler where maximum particle distribution is maintained with less particles outflow of the top of the gas cooler. Vertical internal cooling tubes found better performance compared to horizontal tubes arrangement.

## References

- [1] R. Jaiswal, M. S. Eikeland, B. M. E. Moldestad, and R. K. Thapa, “Influence on the fluidization pattern of a freely bubbling fluidized bed with different modes of air supply,” presented at the 63rd International Conference of Scandinavian Simulation Society, SIMS 2022, Trondheim, Norway, September 20-21, 2022, Oct. 2022, pp. 291–296. doi: 10.3384/ecp192041.
- [2] Y. Zhang and Q. Wei, “CPFD simulation of bed-to-wall heat transfer in a gas-solids bubbling fluidized bed with an immersed vertical tube,” *Chem. Eng. Process. Process Intensif.*, vol. 116, pp. 17–28, Jun. 2017, doi: 10.1016/j.cep.2017.03.007.
- [3] J. C. Chen, J. R. Grace, and M. R. Golriz, “Heat transfer in fluidized beds: design methods,” *Powder Technol.*, vol. 150, no. 2, pp. 123–132, Feb. 2005, doi: 10.1016/j.powtec.2004.11.035.
- [4] C. Wu, H. Yang, X. He, C. Hu, L. Yang, and H. Li, “Principle, development, application design and prospect of fluidized bed heat exchange technology: Comprehensive review,” *Renew. Sustain. Energy Rev.*, vol. 157, p. 112023, Apr. 2022, doi: 10.1016/j.rser.2021.112023.
- [5] L. P. Hatch, G. G. Weth, and S. J. Wachtel, “Scale control in the high temperature distillation of saline waters by means of fluidized-bed heat exchangers,” *Desalination*, vol. 1, no. 2, pp. 156–164, Jul. 1966, doi: 10.1016/S0011-9164(00)84015-1.
- [6] C. A. Allen, E. S. Grimmer, and R. McAtee, “The development of liquid-fluidized bed heat exchangers for controlling the deposition of scale in geothermal applications,” Idaho National Engineering Laboratory, Idaho Falls, ID, COO-2607-4; CONF-760844-17, Jan. 1976. Accessed: Apr. 16, 2024. [Online]. Available: <https://www.osti.gov/biblio/886877>
- [7] D. T. J.M. Wheeldon, “Bubbling Fluidized Bed - an overview | ScienceDirect Topics.” Accessed: May 02, 2024. [Online]. Available: <https://www.sciencedirect.com/topics/engineering/bubbling-fluidized-bed>
- [8] “Aluminium,” IEA. Accessed: May 29, 2024. [Online]. Available: <https://www.iea.org/energy-system/industry/aluminium>
- [9] H. K. Versteeg and W. Malalasekera, *An introduction to computational fluid dynamics: the finite volume method*, 2. ed., [Nachdr.]. Harlow: Pearson/Prentice Hall, 2007.
- [10] D. Kunii and O. Levenspiel, *Fluidization engineering*. Butterworth-Heinemann, 1991.
- [11] K. G. Palappan and P. S. T. Sai, “Studies on segregation of binary mixture of solids in continuous fast fluidized bed: Part II. Effect of particle size,” *Chem. Eng. J.*, vol. 139, no. 2, pp. 330–338, Jun. 2008, doi: 10.1016/j.cej.2007.08.003.
- [12] R. Cocco, S. Karri, and T. Knowlton, “Introduction to Fluidization,” *Chem. Eng. Prog.*, vol. 110, pp. 21–29, Nov. 2014.
- [13] C. Dechsiri, *Particle Transport in Fluidized Beds: Experiments and Stochastic Models*. Groningen: s.n., 2004.
- [14] R. Sakthivel, G. V. Harshini, M. S. Vardhan, A. Vinod, and K. Gomathi, “3 - Biomass energy conversion through pyrolysis: A ray of hope for the current energy crisis,” in *Green Energy Systems*, V. K. Singh, N. Bangari, R. Tiwari, V. Dubey, A. K. Bhoi, and T. S. Babu, Eds., Academic Press, 2023, pp. 37–68. doi: 10.1016/B978-0-323-95108-1.00006-9.

- [15] H. S. Mickley and C. A. Trilling, "Heat transfer characteristics of fluidized beds," *Ind. Eng. Chem.*, vol. 41, no. 6, pp. 1135–1147, 1949.
- [16] P. C. Bisognin, J. C. S. Câmara Bastos, H. F. Meier, N. Padoin, and C. Soares, "Influence of different parameters on the tube-to-bed heat transfer coefficient in a gas-solid fluidized bed heat exchanger," *Chem. Eng. Process. - Process Intensif.*, vol. 147, p. 107693, Jan. 2020, doi: 10.1016/j.cep.2019.107693.
- [17] G. Flamant *et al.*, "Dense suspension of solid particles as a new heat transfer fluid for concentrated solar thermal plants: On-sun proof of concept," *Chem. Eng. Sci.*, vol. 102, pp. 567–576, Oct. 2013, doi: 10.1016/j.ces.2013.08.051.
- [18] A. Blaszczyk, M. Pogorzelec, and T. Shimizu, "Heat transfer characteristics in a large-scale bubbling fluidized bed with immersed horizontal tube bundles," *Energy*, vol. 162, pp. 10–19, Nov. 2018, doi: 10.1016/j.energy.2018.08.008.
- [19] P. Mahanta, R. S. Patil, and M. Pandey, "Effect of particle size and sand inventory on wall-to-bed heat transfer characteristics of circulating fluidized bed riser," presented at the Proceedings of the world congress on engineering, Citeseer, 2010.
- [20] M. Ehsani, S. Movahedirad, and S. Shahhosseini, "The effect of particle properties on the heat transfer characteristics of a liquid–solid fluidized bed heat exchanger," *Int. J. Therm. Sci.*, vol. 102, pp. 111–121, Apr. 2016, doi: 10.1016/j.ijthermalsci.2015.11.004.
- [21] P. G. Smith, *Applications of Fluidization to Food Processing*. John Wiley & Sons, 2008.
- [22] A. R. Abrahamsen and D. Geldart, "Behaviour of gas-fluidized beds of fine powders part I. Homogeneous expansion," *Powder Technol.*, vol. 26, no. 1, pp. 35–46, May 1980, doi: 10.1016/0032-5910(80)85005-4.
- [23] A. Haider and O. Levenspiel, "Drag coefficient and terminal velocity of spherical and nonspherical particles," *Powder Technol.*, vol. 58, no. 1, pp. 63–70, May 1989, doi: 10.1016/0032-5910(89)80008-7.
- [24] "Significance of Density Of Powders: Bulk Density Vs. True Particle Density - Microspheres Online." Accessed: May 14, 2024. [Online]. Available: <https://microspheres.us/density-of-powder-bulk-true-particle/>
- [25] "What is density? how to distinguish different density definitions? – Cement Science." Accessed: May 14, 2024. [Online]. Available: <https://www.cementscience.com/2013/03/what-is-density-how-to-distinguish-different-density-definitions.html>
- [26] Gianluca Iaccarino, "Geometry Modeling & Grid Generation," Stanford University, 2004. [Online]. Available: <https://web.stanford.edu/class/me469b/handouts/geoandgrid.pdf>
- [27] D. M. Snider, "An Incompressible Three-Dimensional Multiphase Particle-in-Cell Model for Dense Particle Flows," *J. Comput. Phys.*, vol. 170, no. 2, pp. 523–549, Jul. 2001, doi: 10.1006/jcph.2001.6747.
- [28] F. A. Williams, *Combustion Theory*, 2nd ed. Boca Raton: CRC Press, 2019. doi: 10.1201/9780429494055.
- [29] "4. Global Settings — Barracuda Virtual Reactor User Manual." Accessed: May 15, 2024. [Online]. Available: [https://cpfd-software.com/user-manual/global\\_settings.html#thermal-settings](https://cpfd-software.com/user-manual/global_settings.html#thermal-settings)

- [30] W.-C. Yang, “Handbook of Fluidization and Fluid–Particle System,” *China Particuology*, vol. 1, pp. 137–137, Jul. 2003, doi: 10.1016/S1672-2515(07)60126-2.
- [31] C. Z. L.-S. Fan, “Principles of Gas-Solid Flows,” *Camb. Univ. Press N. Y.*, 1998.
- [32] “6. Particles — Barracuda Virtual Reactor User Manual.” Accessed: May 23, 2024. [Online]. Available: <https://cpfd-software.com/user-manual/particles.html#subsec-drag-model>
- [33] J. C. Bandara, R. Thapa, H. K. Nielsen, B. M. E. Moldestad, and M. S. Eikeland, “Circulating fluidized bed reactors – part 01: analyzing the effect of particle modelling parameters in computational particle fluid dynamic (CPFD) simulation with experimental validation,” *Part. Sci. Technol.*, vol. 39, no. 2, pp. 223–236, Feb. 2021, doi: 10.1080/02726351.2019.1697773.
- [34] “What you need to know about ‘Heat Transfer’ in CFD,” ManchesterCFD Team. Accessed: May 03, 2024. [Online]. Available: <https://www.manchestercfd.co.uk/post/what-you-need-to-know-about-heat-transfer-in-cfd>
- [35] J. M. Smith, “Introduction to chemical engineering thermodynamics,” *J. Chem. Educ.*, vol. 27, no. 10, p. 584, Oct. 1950, doi: 10.1021/ed027p584.3.
- [36] F. P. Incropera, D. P. DeWitt, T. L. Bergman, and A. S. Lavine, Eds., *Principles of heat and mass transfer*, 7. ed., International student version. Hoboken, NJ: Wiley, 2013.

# Appendices

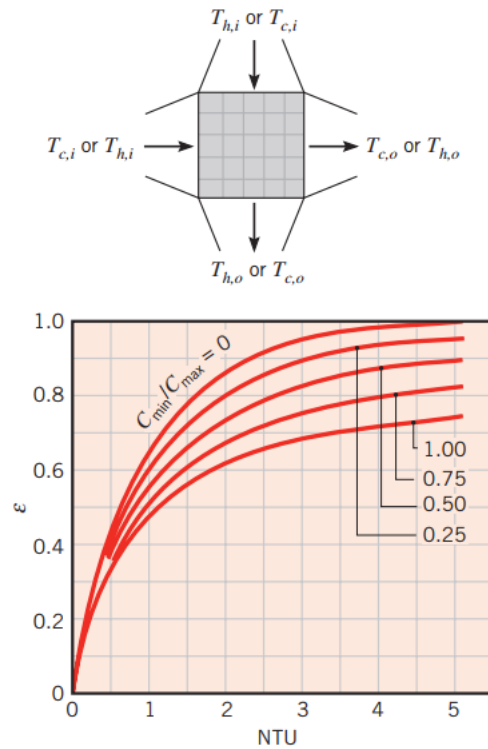
## Appendix A

### Mean diameter calculation of particles.

Quantity in Percentage (%) Cumulative	Diameter in micrometer ( $\mu\text{m}$ )	Actual quantity percentage (%)	Actual quantity	Avarage diameter ( $\mu\text{m}$ )
0	6	0	0	0
0,03	6,21	0,03	0,0003	4,83092E-05
0,06	7,09	0,03	0,0003	4,23131E-05
0,09	9,14	0,07	0,0007	7,65864E-05
0,16	11,79	0,13	0,0013	0,000110263
0,29	15,2	0,26	0,0026	0,000171053
0,55	19,6	0,47	0,0047	0,000239796
1,02	25,27	1,18	0,0118	0,000466957
2,2	32,58	3,17	0,0317	0,00097299
5,37	42,01	7,1	0,071	0,001690074
12,47	54,17	13,49	0,1349	0,002490308
25,96	69,85	20,54	0,2054	0,002940587
46,5	90,06	24,52	0,2452	0,002722629
71,02	116,12	19,19	0,1919	0,001652601
90,21	149,72	7,92	0,0792	0,000528987
98,13	193,04	1,7	0,017	8,80646E-05
99,83	248,9	0,17	0,0017	6,83005E-06
100	320,93	0	0	0
<b>Sum</b>				<b>0,014248348</b>
Mean diameter ( $d_p$ )				70,18357517

## Appendix B

Data chart for calculating NTU for crossflow heat exchangers and gas properties.



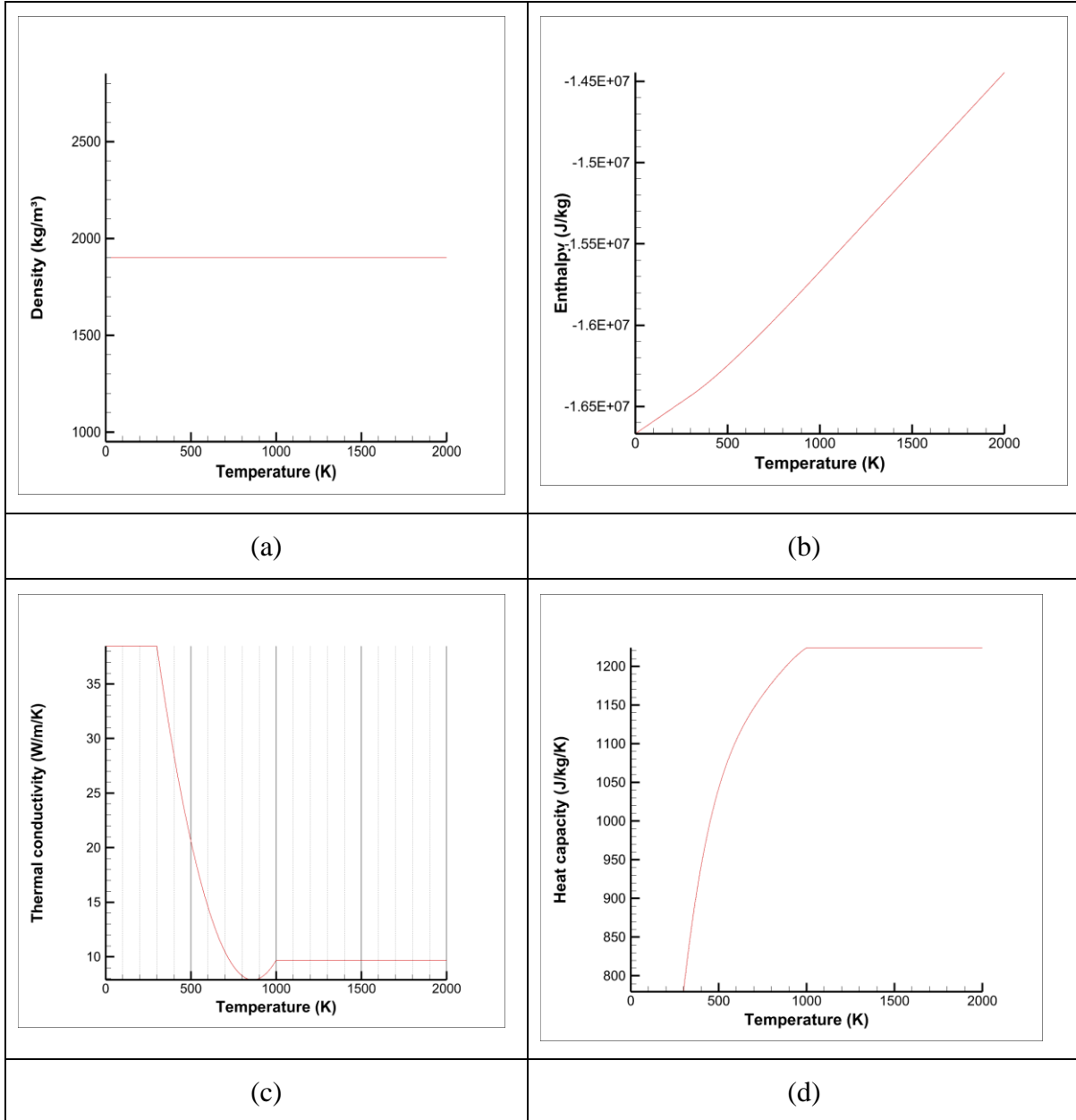
### Thermophysical properties of carbon-di-oxide (CO<sub>2</sub>):

$T$ (K)	$\rho$ (kg/m <sup>3</sup> )	$c_p$ (kJ/kg·K)	$\mu \cdot 10^7$ (N·s/m <sup>2</sup> )	$\nu \cdot 10^6$ (m <sup>2</sup> /s)	$k \cdot 10^3$ (W/m·K)	$\alpha \cdot 10^6$ (m <sup>2</sup> /s)	$Pr$
<b>Ammonia (NH<sub>3</sub>) (continued)</b>							
400	0.5136	2.287	138	26.9	37.0	31.5	0.853
420	0.4888	2.322	145	29.7	40.4	35.6	0.833
440	0.4664	2.357	152.5	32.7	43.5	39.6	0.826
460	0.4460	2.393	159	35.7	46.3	43.4	0.822
480	0.4273	2.430	166.5	39.0	49.2	47.4	0.822
500	0.4101	2.467	173	42.2	52.5	51.9	0.813
520	0.3942	2.504	180	45.7	54.5	55.2	0.827
540	0.3795	2.540	186.5	49.1	57.5	59.7	0.824
560	0.3708	2.577	193	52.0	60.6	63.4	0.827
580	0.3533	2.613	199.5	56.5	63.8	69.1	0.817
<b>Carbon Dioxide (CO<sub>2</sub>), <math>M = 44.01</math> kg/kmol</b>							
280	1.9022	0.830	140	7.36	15.20	9.63	0.765
300	1.7730	0.851	149	8.40	16.55	11.0	0.766
320	1.6609	0.872	156	9.39	18.05	12.5	0.754
340	1.5618	0.891	165	10.6	19.70	14.2	0.746
360	1.4743	0.908	173	11.7	21.2	15.8	0.741
380	1.3961	0.926	181	13.0	22.75	17.6	0.737
400	1.3257	0.942	190	14.3	24.3	19.5	0.737
450	1.1782	0.981	210	17.8	28.3	24.5	0.728
500	1.0594	1.02	231	21.8	32.5	30.1	0.725
550	0.9625	1.05	251	26.1	36.6	36.2	0.721
600	0.8826	1.08	270	30.6	40.7	42.7	0.717
650	0.8143	1.10	288	35.4	44.5	49.7	0.712
700	0.7564	1.13	305	40.3	48.1	56.3	0.717
750	0.7057	1.15	321	45.5	51.7	63.7	0.714
800	0.6614	1.17	337	51.0	55.1	71.2	0.716



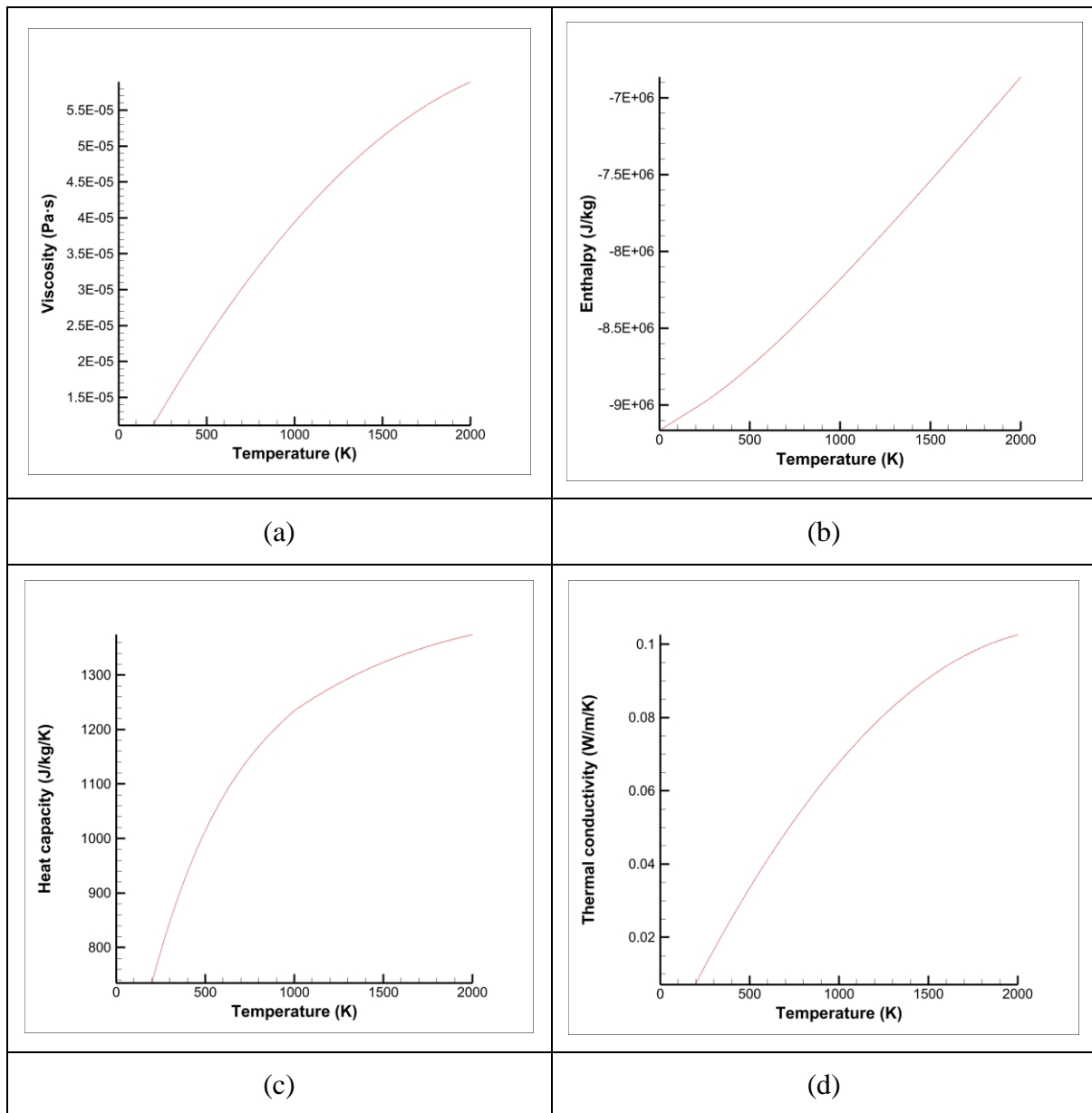
## Appendix C

Alumina particles properties used in CPF D Barracuda VR® (a) density, (b) enthalpy, (c) Thermal conductivity (d) heat capacity.



## Appendix D

Carbon dioxide properties used in CPFV Barracuda VR® (a) viscosity, (b) enthalpy, (c) heat capacity (d) thermal conductivity.



## Appendix E

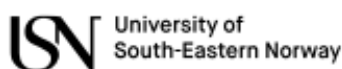
### Particle properties and gas flow conditions provided by Hydro Aluminium AS.

Parameter	Unit	Value
Mean alumina diameter	$\mu\text{m}$	74
Particle envelope density	$\text{kg}/\text{m}^3$	1900
Particle sphericity	-	0.7
Void fraction at minimum fluidization	-	0.442
Particle weight. Fraction. < 45 $\mu\text{m}$	-	0.0894

Parameter	Unit	Value
Inlet gas flowrate	$\text{kg}/\text{h}$	8
Inlet gas pressure	$\text{bar}$	1

## Appendix F

### Task description.



Faculty of Technology, Natural Sciences and Maritime Sciences, Campus Porsgrunn

## FMH606 Master's Thesis

**Title:** CPFDF simulation of fluidized bed-based gas cooler

**USN supervisor:** Chameera Jayarathna

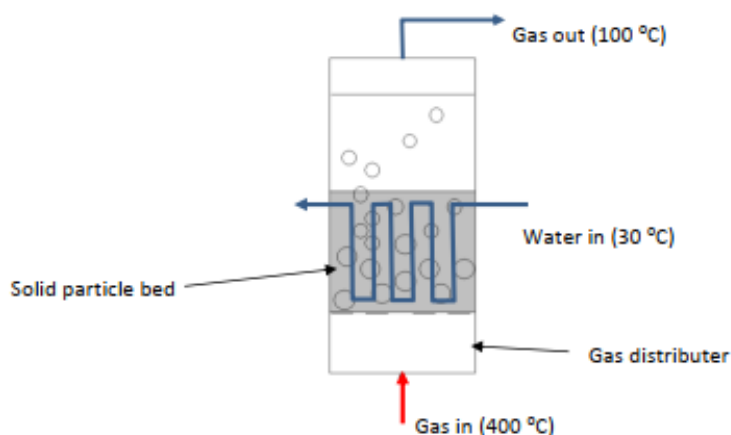
**External partner:** Hydro Aluminium AS (Ron Mangalam Jacob, Burkhard Sachs, etc)

### **Task background:**

Hydro Aluminium AS is one of the leading Aluminium producers in the world. Even though hydro is already low carbon emitter per unit mass of Aluminium they produce, they are continuously working on R & D activities to bring the emission level down. For one of such R & D activities, need a cooler to design to cool down a stream of CO<sub>2</sub> at 400 °C and (at atmospheric pressure) to 100 °C or lower.

### **Task description:**

Based on the nature of the R & D activities, the above-mentioned cooler need to be designed based on the fluidized bed concept. A cooling coil with running cold water should be submerged in the dense part of the fluidized bed, and hot gas is fed from the bottom. Hot gas is then cooled down due to heat transfer between hot gas, solids in the bed, and cooling water. A figure of the concept is shown below.



Following tasks are assumed to be included in the research work.

- A detailed literature study should be done for such a cooler design.
- The geometry size should be calculated based on the gas volume flow rate and the selected fluidization regime. A suitable gas volume flow rate will be discussed.
- The required cooling load and tube length should be calculated, and the mass flow rate of the cooling liquid (water) should be calculated.
- A possible geometry should be considered based on first principal models.
- The CFD model for the case should be made with the CPFDF software Barracuda VR, and the design should be further optimized to maximize the cooling efficiency and minimize the particle entrainment.

**Student category:** EET and PT students who has actively followed the CFD course (PT3110-1) during the autumn semester.

**Is the task suitable for online students (not present at the campus)?** No


**Practical arrangements:**

The student will use a CPFD software called Barracuda VR. USN will provide access to the software.

**Supervision:**

As a general rule, the student is entitled to 15-20 hours of supervision. This includes necessary time for the supervisor to prepare for supervision meetings (reading material to be discussed, etc).

**Signatures:**

Supervisor (date and signature):  23/02/2024

Student (write clearly in all capitalized letters): MD AL-AMIN

Student (date and signature): 